Compositional Optimization and Safety Assessment of a Hydrogel Patch as a Transcutaneous Immunization Device

Kazuhiko MATSUO,[a] Yumiko ISHII,[a] Ying-Shu QUAN,[b] Fumio KAMIYAMA,[b] Hideo ASADA,[c] Yohei MUKAI,[a] Naoki OKADA,*[,a] and Shinsaku NAKAGAWA*[,a]

[a] *Laboratory of Biotechnology and Therapeutics, Graduate School of Pharmaceutical Sciences, Osaka University; 1–6 Yamadaoka, Suita, Osaka 565–0871, Japan:* [b] *CosMED Pharmaceuticals Co., Ltd.; 448–5 Kajii-cho, Kamigyo-ku, Kyoto 602–0841, Japan: and* [c] *Department of Dermatology, Nara Medical University; 480 Shijo-cho, Kashihara, Nara 634–8522, Japan.* Received June 7, 2011; accepted September 8, 2011; published online September 14, 2011

The development of a simple, easy-to-use, and non-invasive vaccination system is in high demand. For transcutaneous immunization (TCI), we previously developed a hydrogel patch formulation that accelerates the penetration of an antigen (Ag) through the stratum corneum (SC) and effectively elicits Ag-specific immune responses. The present studies were performed to optimize the composition and assess the safety of the patch formulation. A hydrogel patch with a water content ratio of 5% more effectively induced an immune response compared to patches with a different composition, suggesting that the moisture content of the hydrogel patch formulation has optimal ratio for SC hydration to promote Ag penetration through the SC. TCI using a hydrogel patch induced few local and systemic adverse reactions. Based on these results, we are now advancing translational research to evaluate the safety and efficacy of our novel TCI system in humans.

Key words transcutaneous immunization; hydrogel patch; composition; skin hydration; safety

Transcutaneous immunization (TCI) is a simple, easy-to-use, and non-invasive vaccination method instead of conventional injection system.[1,2] Langerhans cells (LCs) are the target cells for antigen (Ag) delivery in TCI.[3—7] The top layer of the skin, the stratum corneum (SC), however, acts as a physical barrier to substance penetration.[8] Thus, simply painting an Ag solution onto the skin surface does not allow for Ag delivery to the LCs. To overcome this issue, we developed a hydrogel patch as a TCI device that promotes Ag penetration though the SC.[9] In TCI using a hydrogel patch, Ags are delivered to LCs and Ag-specific immunoglobulin (Ig) G production is induced. The hydrogel patch formulation forms a concentrated Ag layer on its surface, suggesting that the high Ag concentration gradient generated between the patch and the skin tissue by application of the hydrogel patch is critical for producing the driving force necessary to accelerate passive diffusion and distribute the Ags.

Little is known, however, about the optimal composition of the hydrogel patch for the enhancement of Ag penetration through the SC. Reducing the dose of Ag applied to the hydrogel patch is important for production efficiency, and exploring the most appropriate composition for the hydrogel patch is a significant matter for practical application of TCI system using a hydrogel patch. We hypothesized that one of the factors in the hydrogel patch promoting Ag penetration through SC was the induction of SC hydration by hydrogel patch application. In this study, we prepared various hydrogel patches with a different water content to obtain information about the impact of the water content of the hydrogel patch by comparing the Ag-specific IgG production induced by TCI using these patches.

We also assessed the safety of TCI using a hydrogel patch, which is crucial for the clinical use of this vaccination system. In the TCI system, it is feared that skin irritation, such as contact hypersensitivity, might be induced by frequent application of a patch formulation. In the present study, we evaluated adverse reactions at the patch application site and systemic toxicity induced by a hydrogel patch containing excess tetanus and diphtheria toxoids. These studies were performed to obtain the information necessary to proceed to clinical trials of TCI using a hydrogel patch.

MATERIALS AND METHODS

Antigens Ovalbumin (OVA, Sigma-Aldrich Inc., St. Louis, MO, U.S.A.) was used as a model Ag to evaluate the optimal patch formulation. Tetanus and diphtheria toxoids (kindly provided by The Research Foundation for Microbial Diseases of Osaka University, Suita, Japan) were used as practical Ags to evaluate the toxicity of the hydrogel patch formulation.

Animals Male and female hairless rats (5 weeks old), female ddY mice (7 weeks old), and male Wistar rats (5 weeks old) were purchased from SLC Inc. (Hamamatsu, Japan). Animals were handled in accordance with the Osaka University guidelines for experimental animal welfare. The research protocols described in this report were reviewed and approved by the Animal Care and Use Committee of Osaka University.

Patch Formulation for TCI. Four Types of Patches Were Prepared Using the Following Methods (i) Hydrogel Patch (Water Content Ratio; 5%): The hydrophilic adhesive matrix comprised crosslinked HiPAS™ acrylic adhesive (CosMED Pharmaceutical Co., Ltd., Japan), octyldodecyl lactate, glycerin, and sodium hyaluronate. The coating solution was prepared by dissolving the above components in an ethyl acetate/acetone/water mixture, and the matrix was prepared by casting the above mixture solution on a polyester release liner using a knife coater. The solution was allowed to stand at room temperature for 30 min, and then oven-dried at 80 °C for 15 min to remove residual organic solvents. The dried film was then laminated onto a polyester film.

(ii) Hydrophobic Adhesive Patch (Water Content Ratio; 0%): The hydrophobic adhesive matrix consists of crosslinked MASCOS 10™ acrylic adhesive (CosMED Pharmaceutical Co., Ltd., Japan) and isopropyl myristate. The coating solution was prepared by dissolving the above

* To whom correspondence should be addressed. e-mail: okada@phs.osaka-u.ac.jp; nakagawa@phs.osaka-u.ac.jp

components in ethyl acetate, and the matrix was prepared by casting the above mixture solution on a polyester release liner using a knife coater. The solution was allowed to stand at room temperature for 30 min, and subsequently oven-dried at 80 °C for 15 min to remove residual organic solvents. The dried film was then laminated onto polyester film.

(iii) Water-Soluble Adhesive Patch (Water Content Ratio; 66%): The water-soluble adhesive solution comprised sodium acrylate polymer and gelatin, glycerin, and water (8 g : 1 g : 25 g : 56 g). A crosslinker solution was prepared separately by dissolving 0.5 g dihydroxyalumimun aminoacetate in 10 g of 5% sodium tartrate solution. After mixing the crosslinker and adhesive solutions, the matrix was prepared by casting the above mixture solution onto a polyester release liner using a knife coater. The film was then laminated onto polyester non-woven fabric and allowed to stand at room temperature overnight.

Fifty microliters of the Ag solution was dropped onto the surface of each patch. The patches were applied soon after water absorption or, in some cases, after storage at 37 °C for 8 h, and at 4 °C or 25 °C for 1 month or 6 month.

(iv) Dry Gauze and Wet Gauze Patches: Fifty microliters of the Ag solution was dropped onto gauze. For TCI, the Ag-containing gauze was applied either before drying (wet gauze patch) or after drying (dry gauze patch).

Vaccination Protocol and Antibody Titer Measurement Each patch formulation (2 cm^2) containing 100 μg OVA was applied to the auricle of ddY mice for 24 h. The patches were covered with wound management film (BIOCLUSIVE; Johnson & Johnson Medical, Ltd., Tokyo, Japan) to allow for better skin adherence. The procedure was repeated 2 weeks later. As a positive control, an intradermal immunization group comprised mice that were intradermally injected with 100 μg OVA using the same procedure. Two weeks after the final vaccination, sera were collected from the mice and the OVA-specific antibody titer was determined using an enzyme-linked immunosorbent assay (ELISA). End-point titers of OVA-specific antibody are expressed as the reciprocal $\log_2$ of the last dilution that showed 0.1 absorbance units after subtracting the background, as described previously.[9,10]

Measurement of Skin Surface Impedance after Hydrogel Patch Application The abdominal skin of Wistar rats was shaved the day before the experiment. The hydrogel patch (water content ratio; 5%) or filter paper patch containing OVA (100 μg/2 cm^2 each) was applied to the shaved skin. Twenty-four hours later, the patches were removed and the skin surface impedance between the patch application area and the non-application skin area was measured within 30 s using a Pocket Tester (CDM-03D; Custom Inc., Kanagawa, Japan). The impedance of the skin is defined as the resistance measurement between two electrodes in electrical contact with the epidermis.[11]

Histopathologic Image of Human Skin after Application of the Hydrogel Patch A hydrogel patch (1 cm^2) was applied to human skin in the donor component of a Frantz cell system for 24 h. As a control, phosphate-buffered saline (PBS) was applied to human skin. The human skin was removed, fixed in 10% neutral formalin buffer, and embedded in paraffin. The histopathologic changes of human skin at the application site were examined using hematoxyin and eosin (HE)-stained specimens.

Release Test of Ag Contained on Hydrogel Patch OVA-containing hydrogel patch (200 μg/2 cm^2) was prepared. These patches were sealed off and preserved at 4 or 25 °C for 7, 35, or 105 d. After preservation, OVA-containing patches were agitated and sonicated in deionized water. Amount of OVA in obtained supernatant was detected by gel filtration chromatography. Indicated data express as average of two.

***In Vivo* Toxicity Evaluation of Ag-Containing Hydrogel Patch** Four types of hydrogel patches (water content ratio; 5%) containing combined tetanus and diphtheria toxoids in various doses (0, 50, 200, or 400 μg each/cm^2) were applied to the back skin of individual hairless rat for 24 h four times (Fig. 3A). The patches were covered with wound management film to allow for better skin adherence. As a control group, wound management film alone was applied to the back skin of hairless rats.

Body weight was monitored during this time. On day 23, the test sites were observed immediately after removal of the hydrogel patch and scored for signs of erythema or edema according to the Draize dermal scoring criteria.[12] This scale is used to assess irritation as follows: 0, no erythema or edema; 1, very slight erythema and/or barely perceptible edema; 2, well-defined erythema and/or slight edema; 3, moderate to severe erythema or moderate edema; and 4, severe erythema and/or edema. Also, on day 23, serum, skin, liver, kidney, spleen, and lymph nodes were collected from hairless rats, and then weights of harvested liver, kidney, and spleen were measured. Each tissue (skin, liver, kidney, spleen, and lymph node) was fixed in 10% neutral-buffered formalin at pH 7.4 (Wako Pure Chemical Industries, Ltd., Osaka, Japan) and embedded in paraffin. Sections (5 μm) were prepared for HE staining. Histopathologic examinations were performed at the Applied Medical Research Laboratory (Osaka, Japan). Inflammation level was scored according to the severity of the inflammatory cell infiltration: 0, none; 1, rare; 2, mild; 3, moderate; 4, severe. Scoring was performed by an investigator masked to the treatment condition to avoid bias. In addition, a commercial kit was used for quantitative colorimetric determination of glutamic-oxalacetic transaminase (GOT), glutamic-pyruvic transaminase (GPT), and creatinine (CRE) (Transaminase-CII-Test-Wako and Creatinine-test-Wako, respectively; all purchased from Wako Pure Chemical Industries) from rat serum.

RESULTS AND DISCUSSION

Ag-Specific IgG Production Induced by TCI Using Various Patches We previously revealed that the hydrogel patch was an effective vaccine device for TCI.[9,10] Other groups have reported that TCI using gauze patch as the TCI device also induces Ag-specific immune responses.[13] We compared the immune response induced by TCI using either dry gauze patch, wet gauze patch, or the hydrogel patch. TCI using wet gauze patch, but not dry gauze patch, induced an OVA-specific immune response (Fig. 1A), suggesting that SC hydration caused by application of wet gauze patch promoted Ag penetration through the SC. TCI using the hydrogel patch, however, induced a larger immune response. We previously revealed that the hydrogel patch formulation forms a concentrated Ag layer on its surface, and hypothesized that

the high Ag concentration gradient generated between the patch and the skin tissue by application of the hydrogel patch is critical for producing the driving force necessary to accelerate passive diffusion and distribution of the Ags.[9] Because the hydrogel patch is an airtight structure as compared with a wet gauze patch, we speculated that application of the hydrogel patch would restrict water evaporation from the skin, increase the hydration of the SC, and thus promote Ag penetration through the SC, which would more efficiently induce Ag-specific IgG production.

Therefore, to explore the most appropriate water content ratio of the patch formulation, which might determine the degree of SC hydration, we prepared three types of patch formulations with different water content ratios (0%; hydrophobic adhesive patch, 5%; hydrogel patch, and 66%; water-soluble adhesive patch). Mice vaccinated using a hydrogel patch (water content ratio: 5%) had the highest serum anti-OVA IgG titer (Fig. 1B), suggesting that there is an optimal water content level for the hydrogel patch to induce Ag penetration into the skin. Generally, it appeared that the amount of Ag penetrating the SC would increase if the SC were more hydrated. A patch formulation with too much water might impede distribution of the antigenic proteins into the skin, because the SC comprises mainly lipophilic components. Therefore, a hydrogel patch with a water content ratio of 5%, which induced the largest immune response, was used in the subsequent experiments.

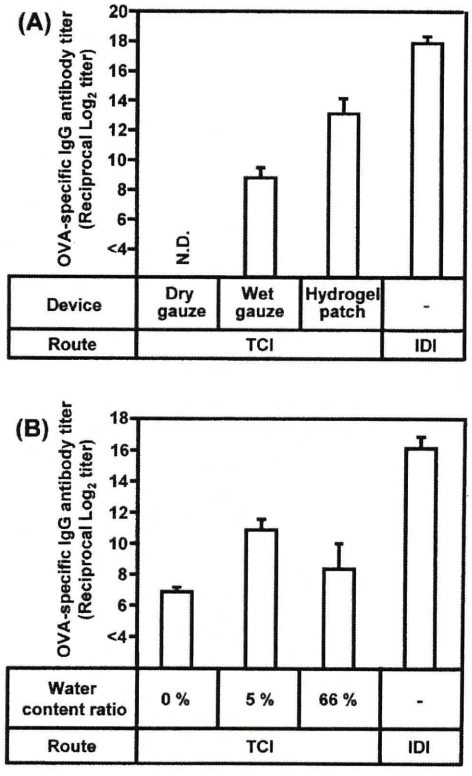

Fig. 1. The Comparison of Ag-Specific IgG Antibody Production Induced by TCI Using Various Patches

(A) Dry gauze patch, wet gauze patch, or a hydrogel patch, (B) the three types of hydrogel patches with a different water content ratio (0%, 5%, or 66%), containing 100 μg OVA, were prepared. These patches were applied to the auricle skin of mice for 24 h. As a control group, mice were intradermally injected with 100 μg OVA. These procedures were performed twice with a 2-week interval. Two weeks after the final vaccination, the serum was collected from these mice and assayed for the OVA-specific IgG titer by ELISA. The results are expressed as means±S.E. of 3 to 7 mice. N.D.; not detectable, TCI; transcutaneous immunization, IDI; intradermal immunization.

Hydration and Humectation of Skin after Hydrogel Patch Application To analyze the hydration effect of SC caused by Ag-containing hydrogel patch application, we measured skin surface impedance after patch application. Surface impedance of skin with application of the hydrogel patch was far lower than that of skin without the patch (Table 1), suggesting that the SC of skin applied with the hydrogel patch was hydrated. In addition, SC swelling was observed in resected human skin following 24 h-application of the hydrogel patch, but not by the application of phosphate-buffered saline (Fig. 2). Thus, hydrogel patch application caused hydration and swelling of SC. In hydrated SC, intercellular gaps are loose and substances are more likely to penetrate into the skin.[14,15] Therefore, by this mechanism, TCI using a hydrogel patch could accelerate Ag penetration through the SC and induce an effective immune response.

Pharmaceutical Stability of the Hydrogel Patch Formulation To investigate the stability of the Ag-containing hydrogel patch, we compared the production of Ag-specific IgG

Table 1. Impedance of Skin Surface on Rat Abdomen

	Skin surface impedance (MΩ·cm)
Intact skin	4.15
Hydrogel patch-applied skin	0.01
Filter paper-applied skin	5.80

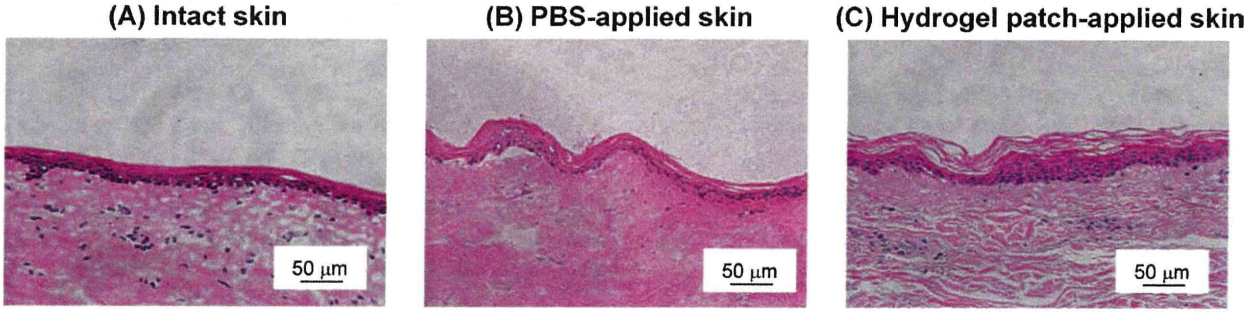

Fig. 2. Histopathologic Image of Human Skin after Application of the Hydrogel Patch

A hydrogel patch was applied to human skin in the donor component of a Frantz cell system for 24 h. As a control, PBS was applied to human skin. The human skin was removed, fixed in 10% neutral formalin buffer, and embedded in paraffin. The histopathologic changes of human skin at the application site were examined using HE-stained specimens.

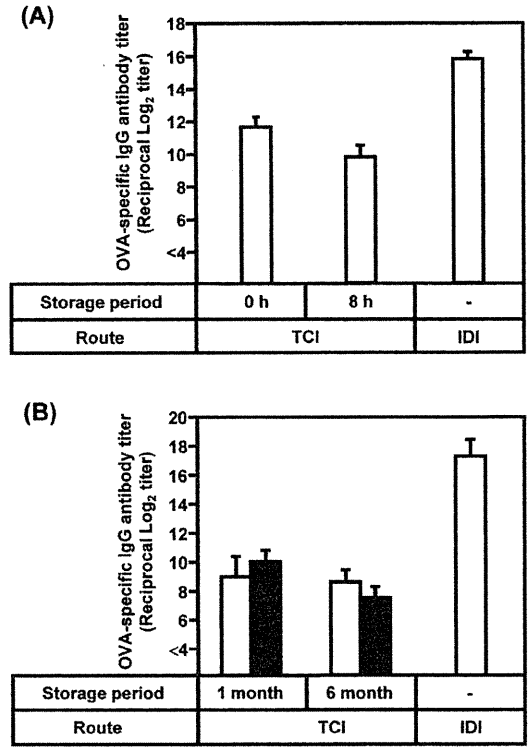

Fig. 3. Evaluation about Long-Term Storage of Ag-Containing Hydrogel Patch

Mice were vaccinated with the two types of hydrogel patches containing 100 μg OVA, which were used for TCI immediately after preparation or after 8 h storage at 37 °C (A), or four types of hydrogel patch containing 100 μg OVA, which were stored for 1 or 6 months at 4 °C (□) or 25 °C (■) (B). As a control group, mice were intradermally injected with 100 μg OVA. These procedures were performed twice with a 2-week interval. Two weeks after the final vaccination, the serum was collected from these mice and assayed for the OVA-specific IgG titer by ELISA. The results are expressed as means±S.E. of 3 to 8 mice. TCI; transcutaneous immunization, IDI; intradermal immunization.

antibody induced by application of hydrogel patch immediately after preparation or after storing the patch for 8 h at 37 °C. TCI using a hydrogel patch stored for 8 h at 37 °C induced an immune response equivalent to that induced by a hydrogel patch used immediately after preparation (Fig. 3A), suggesting that the Ag contained on the hydrogel patch was relatively stable as vaccine-Ag for 8 h. Next, to examine whether Ag-containing hydrogel patch formulation could be preserved under room temperature, we compared the Ag-specific IgG production induced by TCI using hydrogel patch stored under 4 °C and 25 °C for a long period. TCI using a hydrogel patch stored at 25 °C induced an immune response, comparable to that at 4 °C for 1 or 6 months (Fig. 3B). Furthermore, OVA contained on the hydrogel patch kept stable for at least 3 months at 25 °C after preparation as well as at 4 °C (Table 2). These results suggested that Ag-containing hydrogel patch formulation could keep at room temperature without cold chain. This is where our TCI system using a hydrogel patch has advantage over injection vaccine system which must require the use of the cold chain.

Based on these results, TCI using a hydrogel patch formulation (water content ratio; 5%) could induce an Ag-specific immune response most effectively when Ag penetration through the SC is enhanced by hydrating the skin. For practical application, the establishment of a manufacturing method

Table 2. Release Test of Antigenic Protein Contained on Hydrogel Patch

Storage temperature (°C)	Ratio of release amount to contained amount (%)		
	7[a)]	35[a)]	105[a)]
4	108	115	107
25	112	110	105

a) Storage period (Days).

of the hydrogel patch that follows Good Manufacturing Practice is essential and is currently underway.

Toxicity Assessment of TCI Using a Toxoid-Containing Hydrogel Patch For the development of clinical trials, it is crucial to evaluate the side effects caused by application of the Ag-containing hydrogel patch in an animal model. We investigated local irritation on the skin and systemic adverse reactions in hairless rats after applying hydrogel patches containing combined tetanus and diphtheria toxoids with various doses per patch unit area according to the schedule shown in Fig. 4A.

To examine local toxicity, we evaluated erythema and edema at the patch application site using Draize scoring after the final application of the hydrogel patches (Fig. 4B). No edema was observed in any rats (data not shown) and in some rats, slight erythema that quickly resolved was observed on the skin applied with the hydrogel patch. Wound management film alone, which is used in clinical practice, however, also induced slight erythema. There were no differences in the degree of erythema between hydrogel patches containing various doses of toxoids (0, 50, 200, 400 μg/cm^2). These results suggest that the toxoid dose contained on the hydrogel patch did not relate to the degree of erythema, and that physical irritation by the adhesive patch or tape application itself caused this erythema. The erythema disappeared within 1 h after removal of each toxoid-containing hydrogel patch, indicating that the degree of skin irritation caused by the hydrogel patch application was a very mild and temporary reaction. In the histopathologic observation, the inflammation score was low in most rats, but moderate inflammatory cell infiltration was observed in some rats with application of the toxoid-containing hydrogel patch as well as with application of the wound management film (Fig. 4C). This phenomenon might also be a result of physical irritation by the adhesive patch or tape application, as described above. These results of the local toxicity test were similar between males and females. Thus, the toxoid-containing hydrogel patch caused little irritation and inflammation to the skin. Furthermore, we estimate that the infiltration of lymphocytes induced by application of the Ag-containing hydrogel patch promoted the activation of immunocompetent cells in the skin.

We then investigated the systemic side effects caused by TCI using a toxoid-containing hydrogel patch. The body weight change in rats with application of the toxoid-containing hydrogel patch followed a pattern similar to that of rats with application of the wound management film alone (Fig. 4D). There were also no significant changes in serum GOT, GPT, or CRE levels in rats with the toxoid-containing hydrogel patch compared to the control group (Fig. 4E). Moreover, there was no difference in organ weights between the two

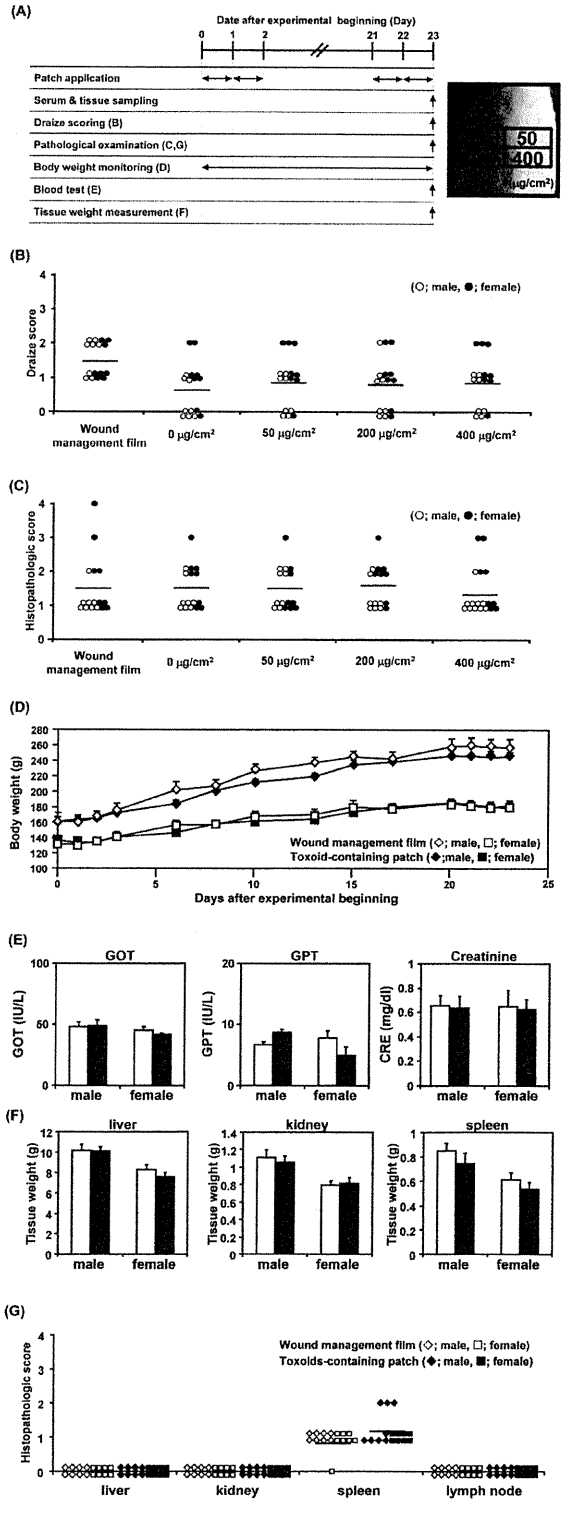

Fig. 4. Local and Systemic Toxicity by TCI Using a Toxoid-Containing Hydrogel Patch

(A) The experimental schedule. A hydrogel patch containing various doses of combined tetanus and diphtheria toxoids (0, 50, 200, or 400 μg each/cm^2) was applied to hairless rats for 24 h, four times. Each experiment was conducted at the indicated time points. Numbers in parentheses indicate experimental number (B)—(G). (B) The degree of erythema on the skin of the hairless rats was evaluated by Draize scoring: 0, no erythema or edema; 1, very slight erythema and/or barely perceptible edema; 2, well-defined erythema and/or slight edema; 3, moderate to severe erythema or moderate edema; and 4, severe erythema and/or edema. Mean value is indicated by the bar. (C) The histopathologic score was determined using HE stained specimens. Lymphocyte infiltration was expressed as follows: 0, no; 1, rare; 2, mild; 3, moderate; 4, severe. Mean value is indicated by the bar. (D) Body weight of hairless rats with application of the hydrogel patch or wound management film alone was monitored during the experiment. (E) Serum levels of GOT, GPT, or CRE were measured in hairless rats with application of the toxoid-containing hydrogel patch (■) or wound management film alone (□). (F) Weight of liver, kidney, and spleen harvested from hairless rats with application of the hydrogel patch (■) or wound management film alone (□) was measured. (G) Histopathologic scores of liver, kidney, spleen, and lymph node harvested from hairless rats with application of the hydrogel patch or wound management film alone were assigned based on HE-stained sections. Histopathologic changes were expressed as follows: 0, no; 1, rare; 2, mild; 3, moderate; 4, severe Mean value is indicated by the bar. Data are expressed as mean±S.E. of results from 8 rats (D), (E), (F).

groups (Fig. 4F). These results of body weight monitoring, biochemical test, and organ weight measurement were similar to untreated control group in males and females and all were within the normal range (data not shown). The histopathologic scores of liver, kidney, spleen, and lymph nodes after application of the toxoid-containing hydrogel patch were within 0 to 1, and there were no toxic changes in any groups (Fig. 4G). In histopathological analysis on spleen, the score of some male rats was higher than the others, but it may just happened that way, but not sex difference. Thus, the systemic toxicity examinations indicated that application of the toxoid-containing hydrogel patch induced no systemic side effects.

Taken together, these findings indicate that TCI with toxoid-containing hydrogel patch is a non-invasive vaccination method without the local and systemic adverse effects associated with immunization. Clinical trials in healthy volunteers are now being planned.

CONCLUSION

In the present study, we determined the optimal water content ratio for the hydrogel patch formulation, and demonstrated the safety and stability of our original TCI system using the hydrogel patch in an animal model. The efficacy of TCI using an Ag-containing hydrogel patch formulation was previously demonstrated to provide effective protection against infection. Thus, this effective, easy to use, and noninvasive TCI system could play an important role in providing effective vaccination instead of injection. We are now planning translational research in humans to assess the safety and efficacy of TCI using a hydrogel patch containing tetanus and diphtheria toxoids.

Acknowledgments We are grateful to the Research Foundation for Microbial Diseases of Osaka University (Suita, Japan) for providing the tetanus and diphtheria toxoids. This investigation was supported by the Program for Promotion of Fundamental Studies in Health Sciences of the National Institute of Biomedical Innovation (NIBIO), by a Grant-in-Aid from the Mochida Memorial Foundation for Medical and Pharmaceutical Research, and by a Grant-in-Aid from the Tokyo Biochemical Research Foundation.

REFERENCES

1) Kersten G., Hirschberg H., *Expert Opin. Drug Deliv.*, **4**, 459—474 (2007).
2) Azad N., Rojanasakul Y., *Curr. Drug Deliv.*, **3**, 137—146 (2006).
3) Berger C. L., Vasquez J. G., Shofner J., Mariwalla K., Edelson R. L., *Int. J. Biochem. Cell Biol.*, **38**, 1632—1636 (2006).
4) Sugita K., Kabashima K., Atarashi K., Shimauchi T., Kobayashi M., Tokura Y., *Clin. Exp. Immunol.*, **147**, 176—183 (2007).
5) Mathers A. R., Larregina A. T., *Immunol. Res.*, **36**, 127—136 (2006).
6) Metz M., Siebenhaar F., Maurer M., *Immunobiology*, **213**, 251—260 (2008).
7) Goodarzi H., Trowbridge J., Gallo R. L., *Clin. Rev. Allergy Immunol.*, **33**, 15—26 (2007).
8) Barry B. W., *Nat. Biotechnol.*, **22**, 165—167 (2004).
9) Ishii Y., Nakae T., Sakamoto F., Matsuo K., Matsuo K., Quan Y. S., Kamiyama F., Fujita T., Yamamoto A., Nakagawa S., Okada N., *J. Controlled Release*, **131**, 113—120 (2008).
10) Matsuo K., Ishii Y., Quan Y. S., Kamiyama F., Mukai Y., Yoshioka Y., Okada N., Nakagawa S., *J. Controlled Release*, **149**, 15—20 (2011).
11) Kinnen E., *Med. Electron. Biol. Eng.*, **3**, 67—70 (1965).
12) Draize J. H., Woodard G., Calvery H. O., *J. Pharmacol. Exp. Ther.*, **82**, 377—390 (1944).
13) Naito S., Maeyama J., Mizukami T., Takahashi M., Hamaguchi I., Yamaguchi K., *Vaccine*, **25**, 8762—8770 (2007).
14) Edelberg R., *J. Invest. Dermatol.*, **69**, 324—327 (1977).
15) Alonso A., Meirelles N. C., Yushmanov V. E., Tabak M., *J. Invest. Dermatol.*, **106**, 1058—1063 (1996).

OPEN ACCESS Freely available online

PLoS one

Requirement of Interaction between Mast Cells and Skin Dendritic Cells to Establish Contact Hypersensitivity

Atsushi Otsuka[1,2], Masato Kubo[3], Tetsuya Honda[1], Gyohei Egawa[1], Saeko Nakajima[1], Hideaki Tanizaki[1], Bongju Kim[2], Satoshi Matsuoka[2], Takeshi Watanabe[2], Susumu Nakae[4], Yoshiki Miyachi[1], Kenji Kabashima[1]*

1 Department of Dermatology, Kyoto University Graduate School of Medicine, Kyoto, Japan, **2** Center for Innovation in Immunoregulative Technology and Therapeutics, Kyoto University Graduate School of Medicine, Kyoto, Japan, **3** Laboratory for Signal Network, Research Center for Allergy and Immunology, RIKEN Yokohama Institute, Tsurumi, Yokohama, Kanagawa, Japan, **4** Frontier Research Initiative, Institute of Medical Science, University of Tokyo, Minato, Tokyo, Japan

Abstract

The role of mast cells (MCs) in contact hypersensitivity (CHS) remains controversial. This is due in part to the use of the MC-deficient *Kit* $^{W/Wv}$ mouse model, since *Kit* $^{W/Wv}$ mice congenitally lack other types of cells as a result of a point mutation in c-kit. A recent study indicated that the intronic enhancer (IE) for *Il4* gene transcription is essential for MCs but not in other cell types. The aim of this study is to re-evaluate the roles of MCs in CHS using mice in which MCs can be conditionally and specifically depleted. Transgenic Mas-TRECK mice in which MCs are depleted conditionally were newly generated using cell-type specific gene regulation by IE. Using this mouse, CHS and FITC-induced cutaneous DC migration were analyzed. Chemotaxis assay and cytoplasmic Ca^{2+} imaging were performed by co-culture of bone marrow-derived MCs (BMMCs) and bone marrow-derived dendritic cells (BMDCs). In Mas-TRECK mice, CHS was attenuated when MCs were depleted during the sensitization phase. In addition, both maturation and migration of skin DCs were abrogated by MC depletion. Consistently, BMMCs enhanced maturation and chemotaxis of BMDC in ICAM-1 and TNF-α dependent manners Furthermore, stimulated BMDCs increased intracellular Ca^{2+} of MC upon direct interaction and up-regulated membrane-bound TNF-α on BMMCs. These results suggest that MCs enhance DC functions by interacting with DCs in the skin to establish the sensitization phase of CHS.

Citation: Otsuka A, Kubo M, Honda T, Egawa G, Nakajima S, et al. (2011) Requirement of Interaction between Mast Cells and Skin Dendritic Cells to Establish Contact Hypersensitivity. PLoS ONE 6(9): e25538. doi:10.1371/journal.pone.0025538

Editor: Nirbhay Kumar, Tulane University, United States of America

Received May 12, 2011; **Accepted** September 6, 2011; **Published** September 30, 2011

Funding: This work was supported in part by Grants-in-Aid for Scientific Research from the Ministry of Education, Culture, Sports, Science and Technology of Japan. The funders had no role in study design, data collection and analysis, decision to publish, or preparation of the manuscript. No additional external funding received for this study.

Competing Interests: The authors have declared that no competing interests exist.

* E-mail: kaba@kuhp.kyoto-u.ac.jp

Introduction

Contact hypersensitivity (CHS) has been widely used to study cutaneous immune responses, since it is a prototype of delayed-type hypersensitivity mediated by antigen -specific T cells [1,2,3,4]. An essential step in the sensitization phase for CHS is the migration of hapten-bearing cutaneous dendritic cells (DCs), such as epidermal Langerhans cells (LCs) and dermal DCs, into skin-draining lymph nodes (LNs). After completing their maturation, mature DCs present antigen to naive T cells in the LNs, thus establishing the sensitization phase. In the subsequent challenge phase, re-exposure to the cognate hapten results in the recruitment of antigen-specific T cells and other non-antigen-specific leukocytes.

The functions of cutaneous DCs are modulated by keratinocyte-derived proinflammatory cytokines [1,5]. The role of the different skin DC subsets in CHS (inducers, regulators, or functional redundancy) is a matter of active debate [6]. In addition, dermal DCs, including Langerin $(CD207)^+$ dermal DCs, may also play an important role in CHS [7,8].

Mast cells (MCs) are a candidate DC modulator since they express and release a wide variety of intermediaries, such as histamine, tumor necrosis factor (TNF)-α and lipid mediators. It has been reported that activated human cord blood-derived MCs induce DC maturation *in vitro* [9], that IgE-stimulated MC-derived histamine induces murine LC migration *in vivo* [10], and that MC-derived TNF-α promotes cutaneous murine DC migration *in vivo* in an IgE-independent manner [11]. On the other hand, prostaglandin (PG) D_2 produced by MCs in response to allergens [12], inhibits LC migration [13]. Therefore, MCs might have bi-directional effects on DC activity in a context-dependent manner and the question of the mechanisms by which DCs are modulated by MCs is an important issue to pursue.

While MCs have been assumed to play an important role in CHS, their role is controversial. Previous studies have demonstrated that MC-deficient *Kit* $^{W/Wv}$ mice show attenuated CHS responses, meanwhile, other studies have shown that CHS was not impaired in *Kit*$^{W/Wv}$ mice [14]. Although some studies indicated that the discrepancy in *W/Wv* mice might be due to the difference in hapten dose, the detailed mechanism is still unclear. *Kit* $^{W/Wv}$ mice and *Kit*$^{W\text{-}sh/KitW\text{-}sh}$ mice have an inversion mutation in the Kit gene [15], and therefore, these mice also lack melanocytes and hematopoietic stem cells, which are known to modulate immune responses [16,17]. In addition, since MCs are congenitally absent, it is possible that compensatory mechanisms may exist that

modulates immune system functions. Therefore, it is important to re-evaluate the roles of MCs using mice in which MCs can be conditionally and specifically depleted.

Recently, we have demonstrated that MCs and basophils use specific enhancer elements, intronic enhancer (IE) and a 3′ 4kb fragment that contains 3′UTR and HS4 elements, to regulate *Il4* gene expression, respectively [18]. Taking advantage of this system, we have generated mice that contain human diphtheria toxin receptor (DTR) under the control of IE. Therefore, mast cell-specific enhancer-mediated Toxin Receptor-mediated Conditional cell Knock out (TRECK) systems were designated as Mas-TRECK transgenic (Tg) mice. In these mice, both MCs and basophils are conditionally depleted by diphtheria toxin (DT) treatment. Since basophils recover much faster than MCs (Fig S1A, B), there exist a period of specific MC depletion. Taking advantage of the system, we have herein demonstrated that activated DCs induce MC activation, which triggers the migration and maturation of DCs via cell-cell contact. This DC-MC interaction plays an essential role in the sensitization phase of CHS.

Results

Suppression of CHS responses in Mas-TRECK Tg mice

Mice expressing the human DTR under the control of IE element (for Mas-TRECK) and 3′UTR element (for basophil-specific enhancer-mediated TRECK systems; Bas-TRECK) in the *Il4* gene locus were generated by a transgenic strategy (Sawaguchi et al. Manuscript in submission). We initially demonstrated that skin MCs were completely depleted in Mas-TRECK Tg mice 5 and 12 days after an intraperitoneal injection of diphtheria toxin (DT) (See **Fig. S1A** in the Online Repository). Although DX5+ FcεRIα+ basophils in the blood were eliminated 5 days after DT treatment in Mas-TRECK Tg mice, basophil numbers recovered in 12 days (**Fig. S1B** in the Online Repository).

To investigate the role of MCs in cutaneous acquired immune responses, we used DNFB-induced CHS as a model. CHS responses were similar between wild type (WT) and Mas-TRECK Tg mice in the absence of DT treatment (205 μm±10.5 vs 212 μm±12.3; average ± SD). In addition, DT treatment itself did not affect the degree of CHS responses in WT mice. On the other hand, when both WT and Mas-TRECK Tg mice were treated with DT and assayed 12 days later, the CHS response in Mas-TRECK Tg mice was much less than that in WT mice (**Fig. 1A**). The ear swelling of WT and Mas TRECK Tg mice was 48.2 (±5.2, SD) μm and 51.3 (±4.8, SD) μ after 72 h, and 15 (±7.29, SD) μm and 40.1 (±6.68, SD) μm after 96 h respectively. Histology of the ears 48 h after the challenge showed considerable lymphocyte infiltration and edema in the dermis of sensitized WT mice; these changes were less apparent in Mas-TRECK Tg mice (**Fig. 1B, *left panel***) and the histological scores [19] in Mas-TRECK Tg mice were lower than those in WT mice (**Fig. 1B, *right panel***). On the other hand, the CHS response was not impaired in ***Kit$^{W/Wv}$*** mice (See **Fig. S2A** in the Online Repository).

In addition, the CHS response in Bas-TRECK Tg mice, which lack only basophils upon treatment with DT, was similar to that of WT mice (See **Fig. S2B** in the Online Repository). The attenuated CHS response in Mas-TRECK Tg mice was confirmed using an additional hapten, oxazolone (**Fig. 1C**) and also at higher hapten doses (See **Fig. S2C** in the Online Repository).

To clarify the action phase of MCs in CHS, we used an adoptive transfer-induced CHS model. Recipients of LN cells from sensitized WT mice showed an enhanced CHS response, whereas the recipients of LN cells from sensitized Mas-TRECK Tg mice showed a markedly inhibited response (**Fig. 1D**). In addition, the recipients of CD90.2+ T cells from sensitized Mas-TRECK Tg mice showed inhibited responses compared to recipients of CD90.2+ T cells from sensitized WT mice (See **Fig. S2D** in the Online Repository). These data indicate that MCs play important roles in establishing CHS during the sensitization phase.

We further evaluated whether the attenuated CHS in Mas-TRECK Tg mice reflected the lack of MCs. WT or Mas-TRECK Tg mice were engrafted in the skin with or without BMMCs 5×10^6 cells in 100 μl/dorsal skin 1 hour before oxazolone sensitization. The numbers of toluidine blue positive mast cells (per field) in the dermis are 40.2 (±5.3, SD) in Mas TRECK Tg mice and 35.3 (±7.2, SD) in B6 wild type mice after one hour injection of BMMC (n = 3) (See **Fig. S2E** in the Online Repository). On the other hand, the number of MCs in the uninjected sites was 10.5 (±3.2, SD) in B6 wild type mice. Five days after sensitization, the skin-draining LN cells of sensitized mice were adoptively transferred intravenously into naive WT recipients and challenged with oxazolone on the ears. The CHS response of recipients of LN cells from sensitized WT mice was not changed by the pre-engraftment of BMMCs into the skin (**Fig. 1E**). On the other hand, the attenuated CHS response of recipients of Mas-TRECK Tg LN cells was fully restored by the pre-engraftment of BMMCs into the skin.

Next we counted the cells infiltrating the skin of WT and Mas-TRECK Tg mice 12 h after challenge with DNFB. The numbers of CD45+ CD3+ CD4+ T cells, CD45+ CD3+ CD8+ T cells, and CD45+ Gr-1high neutrophils after both sensitization and challenge, and that of neutrophils after only challenge were increased in WT mice. But such increment was attenuated in Mas-TRECK Tg mice (See **Fig. S3A** in the Online Repository). Consistent with this result, the mRNA levels of IFN-γ, IL-17 and IL-1β in the skin 12 h after challenge were significantly decreased in Mas-TRECK Tg mice compared to WT mice (See **Fig. S3B** in the Online Repository).

We further analyzed the composition of LN cells after sensitization. Five days after sensitization, the skin-draining LN cells of WT and Mas-TRECK Tg mice were collected. The numbers of CD44+ CD62L+ central memory T cells and CD44+ CD62L- effector memory T cells among CD4+ and CD8+ T cell subsets were less in Mas-TRECK Tg mice than in WT mice (See **Fig. S4A** in the Online Repository). In contrast, the numbers within each subset in the LN without sensitization were comparable between WT and Mas-TRECK Tg mice (See **Fig. S4A** in the Online Repository).

To evaluate of T cell differentiation after sensitization, the skin-draining LN cells from control or DNFB-sensitized WT and Mas-TRECK Tg mice were challenged in the presence or absence of DNBS *in vitro*. The incorporation of ^{3}H-thymidine and the levels of IFN-γ and IL-17 in the culture supernatant in the presence of DNBS were markedly decreased in LN cells from Mas-TRECK Tg mice as compared with those from WT mice (See **Fig. S4B-D** in the Online Repository). The levels of IL-4 in the culture supernatants were below the limit of detection of ELISA (<0.3 pg/mL).

Attenuated DC migration and maturation in the skin-draining LNs of Mas-TRECK Tg mice

An essential step in the sensitization phase for CHS is the migration of hapten-bearing cutaneous dendritic cells (DCs), such as epidermal Langerhans cells (LCs) and dermal DCs, into skin-draining lymph nodes (LNs). Accordingly, to dissect the site of

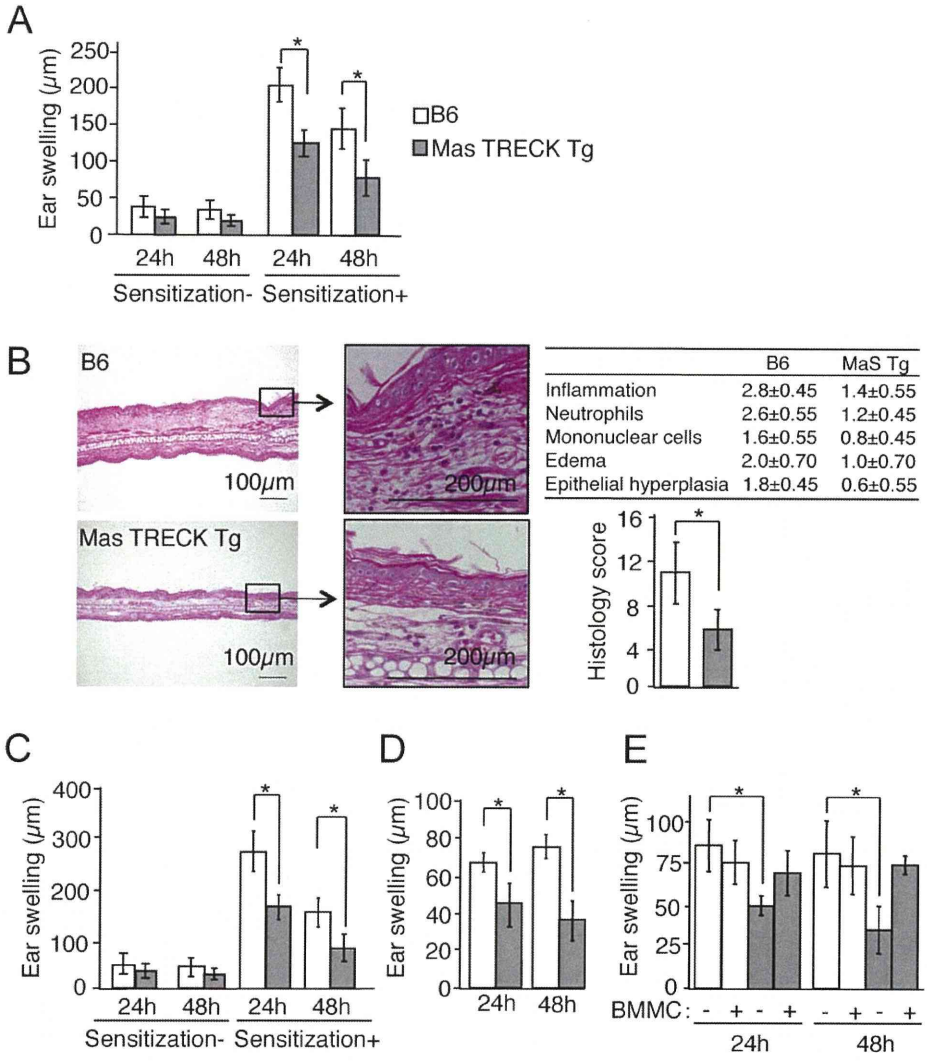

	B6	MaS Tg
Inflammation	2.8±0.45	1.4±0.55
Neutrophils	2.6±0.55	1.2±0.45
Mononuclear cells	1.6±0.55	0.8±0.45
Edema	2.0±0.70	1.0±0.70
Epithelial hyperplasia	1.8±0.45	0.6±0.55

Figure 1. MCs are essential during the sensitization phase in CHS. (A) Twelve days after DT treatment, WT and MaS TRECK Tg mice ($n = 12$ per group) were sensitized with or without DNFB and the ear swelling was measured 24 and 48 h after challenge with DNFB. (B) HE staining of the ears of sensitized DT-treated WT and MaS TRECK Tg mice 24 h after challenge with DNFB. Scale bar, 100 μm (left panels) and 200 μm (middle panels). Samples were scored for the severity and character of the inflammatory response using a subjective grading scale. The total histology score was calculated as the sum of scores (right panels). (C) Oxazolone-induced CHS in WT (white columns) and Mas-TRECK Tg (grey columns) mice. DT-treated WT and MaS TRECK Tg mice ($n = 13$ per group) were sensitized with oxazolone and ear swelling measured 24 and 48 hours after challenge with oxazolone. (D) CHS induced by adoptive transfer of LN cells sensitized with DNFB of WT (white columns) and Mas-TRECK Tg (grey columns) ($n = 6$ per group). (E) Draining LNs from oxazolone-sensitized WT (white columns) and Mas-TRECK Tg (grey columns) reconstituted with BMMCs ($n = 5$ per group) were adoptively transferred to induce CHS. All data are presented as the mean ± SD and are representative of three experiments. *, $P<0.05$ versus corresponding mice.
doi:10.1371/journal.pone.0025538.g001

action of MCs in the sensitization phase, we initially focused on cutaneous DCs that have an opportunity to interact with MCs present in the dermis.

Using a FITC-induced cutaneous DC migration model, we found that the numbers of both FITC$^+$ CD11c$^+$ MHC class II$^+$ CD207$^+$ DCs and FITC$^+$ CD11c$^+$ MHC class II$^+$ CD207$^-$ DCs in the draining LNs 24 h and 72 h after FITC application were significantly attenuated in Mas-TRECK Tg mice compared to WT mice (**Fig. 2A, B**). In addition, the numbers of total CD4$^+$ and CD8$^+$ T cells, and CD44$^+$ CD62L$^+$ central memory and CD44$^+$ CD62L$^-$ effector memory T cells in the draining LNs of Mas-TRECK Tg mice were less than those of WT mice (**Fig. 2C**). We next analyzed the expression levels of costimulatory molecules by skin organ culture. We incubated the skin and analyzed the expression levels on crawl-out DCs in the culture medium. The expression levels of CD40, CD80, and CD86 both on CD11c$^+$ MHC class II$^+$ EpCAM$^+$ LCs and CD11c$^+$ MHC class II$^+$ EpCAM$^-$ dermal DCs in Mas-TRECK Tg mice were lower than those of WT mice (**Fig. 2D, E,** and see **Fig. S5A**, upper panel, in the Online Repository). On the other hand, the expression levels of costimulatory molecules on LCs and dermal DCs from the untreated WT controls and Mas TRECK Tg mice were comparable (See **Fig. S5A**, lower panel, in the Online Repository). In addition, the expression levels on LCs and dermal DCs from WT and Mas-TRECK mice were comparable under steady state conditions (See **Fig. S5B** in the Online Repository).

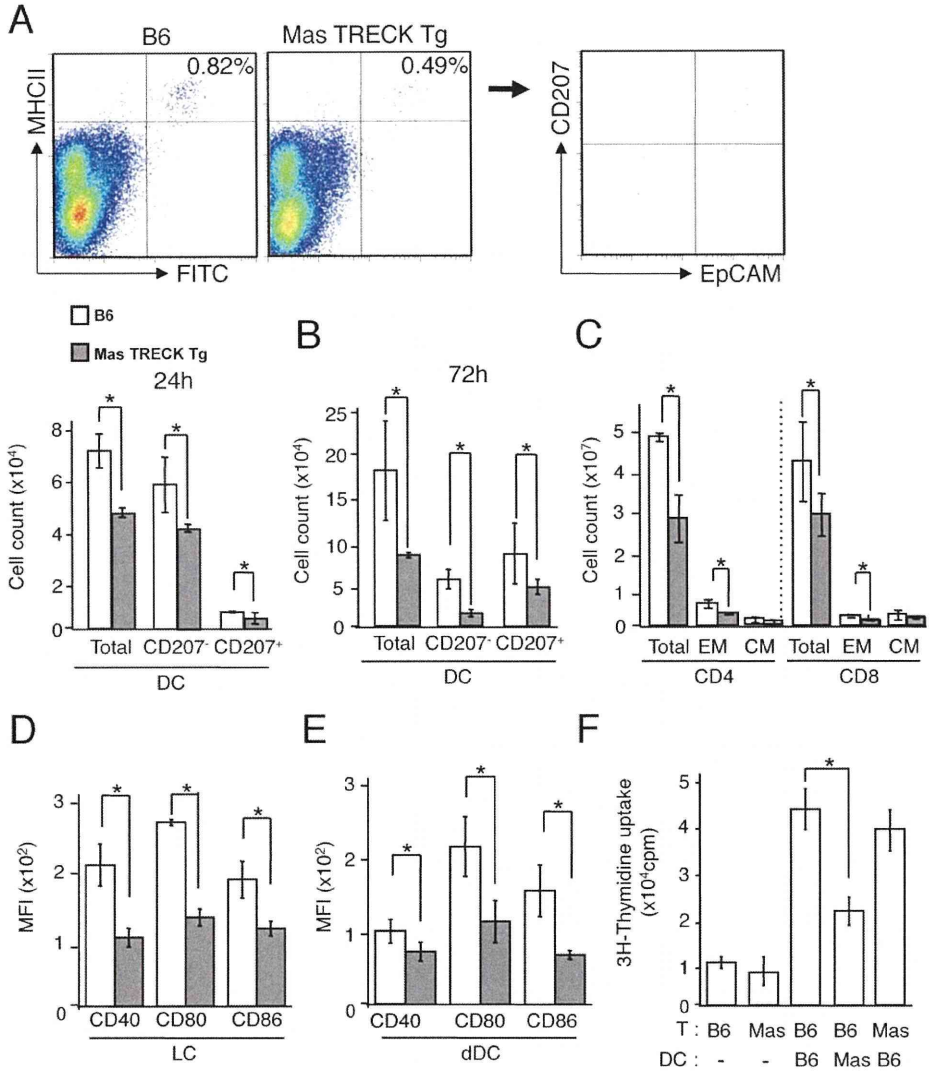

Figure 2. Impaired cutaneous DC migration and maturation in Mas-TRECK Tg mice. (A, B) The numbers of FITC$^+$ CD11c$^+$ MHC class II$^+$ CD207$^+$ DCs and FITC$^+$ CD11c$^+$ MHC class II$^+$ CD207$^-$ DCs in the draining LNs of DT-treated MaS TRECK Tg and WT mice 24 h and 72 h after application of FITC. (**C**) The numbers of total, central memory (CM), and effector memory (EM) CD4$^+$ and CD8$^+$ T cells in the draining LN 72 h after FITC application are shown. (D, E) The expression levels of CD40, CD80, and CD86 on both LCs and dDCs of DT-treated MaS TRECK Tg and WT mice. (F) *In vitro* assay of T-cell proliferation induced by DCs sorted from the draining LN of sensitized mice of WT or Mas-TRECK Tg (Mas) mice. Oxazolone-sensitized CD90.2$^+$ T cells were purified from the draining LNs of WT or Mas-TRECK Tg (Mas) mice 5 d after oxazolone application. T cells (5×10^5 cells) were incubated for 72 h, pulsed with 0.5 μCi [^{3}H]thymidine for the last 24 h ,with or without CD11c$^+$ DCs (1×10^5 cells) prepared from the draining LNs of DT-treated WT and MaS TRECK Tg mice one day after oxazolone application. All data are presented as the mean ± SD and are representative of three experiments. *, $P<0.05$ versus a corresponding group.
doi:10.1371/journal.pone.0025538.g002

Consistently, LCs and dermal DCs from *Kit*+/+ mice were similar to those from *Kit* $^{W/W\text{-}v}$ mice (See **Fig. S5B** in the Online Repository).

We further evaluated the effect of MCs on the antigen presenting capacity of DCs. We sorted 5×10^5 T cells by auto MACS from the draining LNs of CD90.2$^+$ WT mice five days after 25 μl of 2% oxazolone application. These CD90.2$^+$ T cells were incubated for 72 h with or without CD11c$^+$ DCs (1×10^5 cells) prepared from the draining LNs of WT or Mas-TRECK Tg mice one day after oxazolone application. T cell proliferation was enhanced by the addition of antigen-acquired DCs sorted from the draining LN of sensitized mice, and the extent of augmentation by DCs from WT mice was much higher than that of DCs from Mas-TRECK Tg mice (**Fig. 2F**).

Enhancement of BMDC maturation and chemotaxis by BMMC requires cell-cell contact in vitro

Impairment of DC functions as a result of MC deficiency suggests that MCs stimulate cutaneous DCs. To address this hypothesis, we prepared BMDCs [20] and incubated them with or without BMMCs. Co-cultivation of BMDCs with BMMCs for 24 h significantly increased the expression levels of CD40, CD80, CD86 and CCR7 on BMDCs (**Fig. 3A**). In addition the chemotaxis of BMDCs to CCL21 was significantly enhanced,

when BMMCs were added to the upper chamber with BMDCs (**Fig. 3B**).

Furthermore addition of BMMCs to the upper chamber of transwells did not induce further up-regulation of CD40, CD80, CD86 and CCR7 levels on BMDCs incubated in the lower chamber (**Fig. 3C**), which suggests that BMMCs require direct cell-cell interaction to stimulate BMDCs.

Stimulation of BMMCs by activated BMDCs

We then examined *in vitro* whether DCs directly contacted MCs. We incubated BMMCs and BMDCs, and found that c-kit$^+$ BMMCs contacted MHC class II$^+$ BMDCs (**Fig. 4A**). A number of FcεRIα$^+$ CD11c$^-$ MCs co-localized with CD11c$^+$ DCs in ear dermis 24 h after sensitization with DNFB (**Fig. 4B**). Consistent with this, the number of MCs co-located with DCs after sensitization was higher than that in the steady state (in other words, in non-inflammatory conditions) (4±0.81 vs 0.3±0.58; average ± SD).

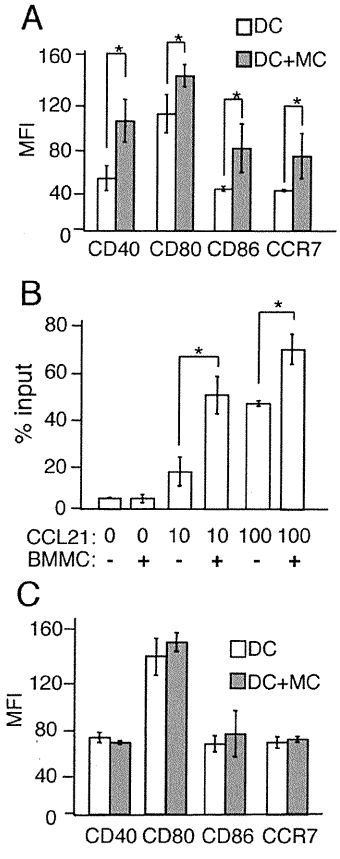

Figure 3. BMMCs promote the maturation and chemotactic activity of BMDCs via direct cell interaction. (A) The expression levels of CD40, CD80, CD86 and CCR7 on BMDCs cultured with or without BMMCs for 24 h. (B) Mobility of BMMCs to CCL21. BMMCs with or without BMDCs were applied to the upper chamber of a transwell without coating for 3 h. The numbers of MHC class II$^+$ cells in the lower chamber, identified as migrating DCs, were counted by means of flow cytometry. (C) The expression levels of CD40, CD80, CD86 and CCR7 on BMDCs cultured with or without BMMCs separately by using transwell culture plates for 24 h. All data are presented as the mean ± SD and are representative of three experiments. *, $P<0.05$ versus a corresponding group.
doi:10.1371/journal.pone.0025538.g003

At present, several stimuli in addition to IgE are known to trigger calcium influx and activate MCs [21]. Therefore, we studied the effect of BMDCs on BMMCs using Ca^{2+} imaging. We incubated tetramethylrhodamine ethyl ester (TMRE)-labeled BMDCs and Fluo-8-labeled BMMCs together. When an intracellular Ca^{2+} concentration of Fluo-8 (green) -labeled BMMCs is upregulated, fluorescence intensity of green becomes increased. Unstimulated CD11c$^+$ MHC class II^{int+} BMDCs did not increase BMMC intracellular Ca^{2+} concentrations (**Fig. 4C,** See **Video S1** in the Online Repository). On the other hand, stimulated CD11c$^+$ MHC class II^{high+} BMDCs induced prominent Ca^{2+} increase in BMMCs (**Fig. 4D** and See **Video S2** in the Online Repository). This rapid rise occurred five to ten times in 1000 seconds, and each spike lasted about 10–20 sec (**Fig. 4E**). Stimulated BMDCs significantly upregulated the ratio of BMMCs with increased Ca^{2+} concentration compared to non-stimulated BMDCs (**Fig. 4F**). These results suggest that stimulated DCs activate MCs via direct cell-cell contact.

Stimulation of DCs by MCs is dependent on ICAM-1-LFA-1 interaction and on MC membrane-bound TNF-α

We then sought to identify how MCs promote DC maturation. It has been reported that ICAM-1 on the surface of MCs directly interacts with leukocyte function-associated antigen 1 (LFA-1) on T cells, and that stimuli such as CD40L, LPS, and TNF-α, upregulate the expression of ICAM-1 on DCs [22]. In fact, the expression of ICAM-1 on BMDCs was up-regulated upon stimulation of BMDCs by LPS and CCL21 (**Fig. 5A**). Therefore, we hypothesized that MCs and DCs interact in an ICAM-1- and LFA-1-dependent manner. Addition of neutralizing anti-ICAM-1 antibody to a culture of BMDCs completely inhibited upregulation of CD40, CD80 and CD86 expression on BMDCs upon addition of BMMC (**Fig. 5B, S6A**).

We then analyzed intracellular signaling using the protein kinase A inhibitor, H89, and the phosphoinositide 3 kinase inhibitor, wortmannin. Although H89 did not inhibit the BMMC-induced upregulation of co-stimulatory molecules on BMDCs, wortmannin inhibited DC maturation (**Fig. 5C, S6B**). These results suggest that binding of ICAM-1 to LFA-1 activates DCs through a PI3-kinase pathway.

Lastly we tried to identify how DCs induce MC activation. TNF-α is first produced as a 26 kDa transmembrane molecule (membrane-bound TNF-α), which is cleaved by the metalloproteinase-disintegrin TNF-α converting enzyme TACE [23] to generate a soluble 17 kDa TNF-α. Studies have shown that membrane-bound TNF-α is also biologically active [24]. We first observed that anti-TNF-α antibody completely blocked DC maturation induced by BMMCs (**Fig. 5B**). Consistently, BMMC from TNF-α KO mice did not promote BMDC maturation (**Fig. S6C**). But the soluble form of TNF-α in the supernatant of co-cultures of BMMCs and TNF-α KO-derived BMDCs was below the detection limit irrespective of BMDC stimulation (<8 pg/ml, each). On the other hand, the level of membrane-bound TNF-α on BMMCs was increased by the addition of BMDCs and even further enhanced when stimulated BMDCs were added (**Fig. 5D**). These results suggest that MCs express membrane-bound TNF-α upon direct interaction with activated DCs through ICAM-1 on DCs and that membrane-bound TNF-α induces expression of co-stimulatory molecules on DCs.

Discussion

In this study, we used Mas-TRECK Tg mice in which MCs can be eliminated specifically and conditionally, and demonstrated

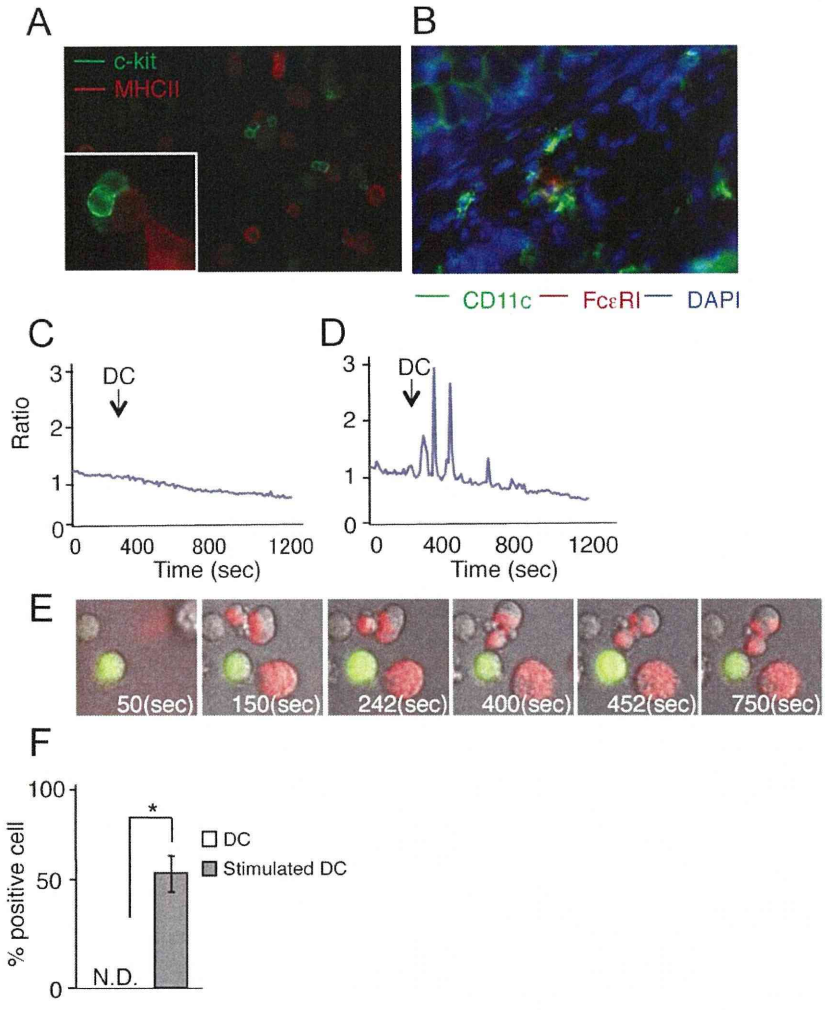

Figure 4. Stimulated BMDCs enhance Ca^{2+} influx in BMMCs and BMMCs interact with DCs in vitro and in vivo. (A) On poly-L-lysine coated glass coverslips, c-kit^{+} BMMCs (green) contacted MHC class II^{+} BMDCs (red). (B) Conjugate formation of CD11c^{+} DCs (green) with FcεRIα^{+} MCs (red) in the sensitized skin. (C–E) BMMCs (green) were co-cultured with non-stimulated BMDCs (C) or BMDCs stimulated with 100 ng/ml of LPS and 50 ng/ml of CCL21 for 1 h (red; D, E), and the intracellular Ca^{2+} was monitored by Fluo-8 for 1200 sec. Photos were taken at the indicated time points from Supplemental Movie 2 (E). (F) The percentage of BMMCs demonstrating high Ca^{2+} concentration among BMMCs. Data are presented as the mean ± SD and are representative of three experiments. *, $P<0.05$ versus a corresponding group.
doi:10.1371/journal.pone.0025538.g004

that CHS was significantly attenuated in accord with impaired memory T cell induction in skin-draining LNs after sensitization. MC depletion also impaired hapten-induced cutaneous DC migration concordant with levels of co-stimulatory molecule expression. In addition, BMMCs promoted BMDC maturation and chemotactic activity by direct interaction via ICAM-1 and membrane-bound TNF-α. In fact, a certain number of DCs were found colocalized with MCs in the DNFB-sensitized dermis. These findings suggest that MCs may promote migration and maturation of dermal DCs and epidermal LCs to establish the sensitization phase of CHS.

It was previously reported that FITC-induced cutaneous DC migration was attenuated in $Kit^{W\text{-}sh/KitW\text{-}sh}$ mice at 24 h, but not at 48 or 72 h after FITC application, and that the sensitization phase of CHS was not attenuated in $Kit^{W\text{-}sh/KitW\text{-}sh}$ mice [11]. The above findings were inconsistent with our findings in the way that cutaneous DC migration was attenuated even at 72 h after FITC application and that sensitization phase was impaired in Mas-TRECK Tg mice. On the other hand, it has also been shown that MCs are capable of influence both the sensitization phase and the elicitation phase in other models of CHS [25]. Therefore, it still remains unknown how the discrepancy occurred. The difference between our model and $Kit^{W/Wv}$ and $Kit^{W\text{-}sh/KitW\text{-}sh}$ mice is the existence of melanocytes and hematopoietic stem cells. Recently, melanocytes were shown to express toll like receptors, to modulate immune responses and to produce IL-1a and IL-1b [16,17]. In addition, because of congenital absence of MCs in $Kit^{W/Wv}$ and $Kit^{W\text{-}sh/KitW\text{-}sh}$ mice, compensatory mechanism may exist, such as repopulation of basophils. In fact, the numbers of basophils have been counted in these mice; the number of basophils in in $Kit^{W/Wv}$ mice are lower than that in WT mice, and that in $Kit^{W\text{-}sh/KitW\text{-}sh}$ mice are higher than that in WT mice [26]. These results indicate that the compensatory mechanisms may affect the result of CHS responses and that $Kit^{W/Wv}$ and $Kit^{W\text{-}sh/KitW\text{-}sh}$ mice may not necessarily be representative to evaluate the roles of pure MCs. In this study, we have demonstrated that the attenuated CHS response in Mas TRECK Tg mice was fully restored by the pre-engraftment of BMMCs into the skin just before sensitization with

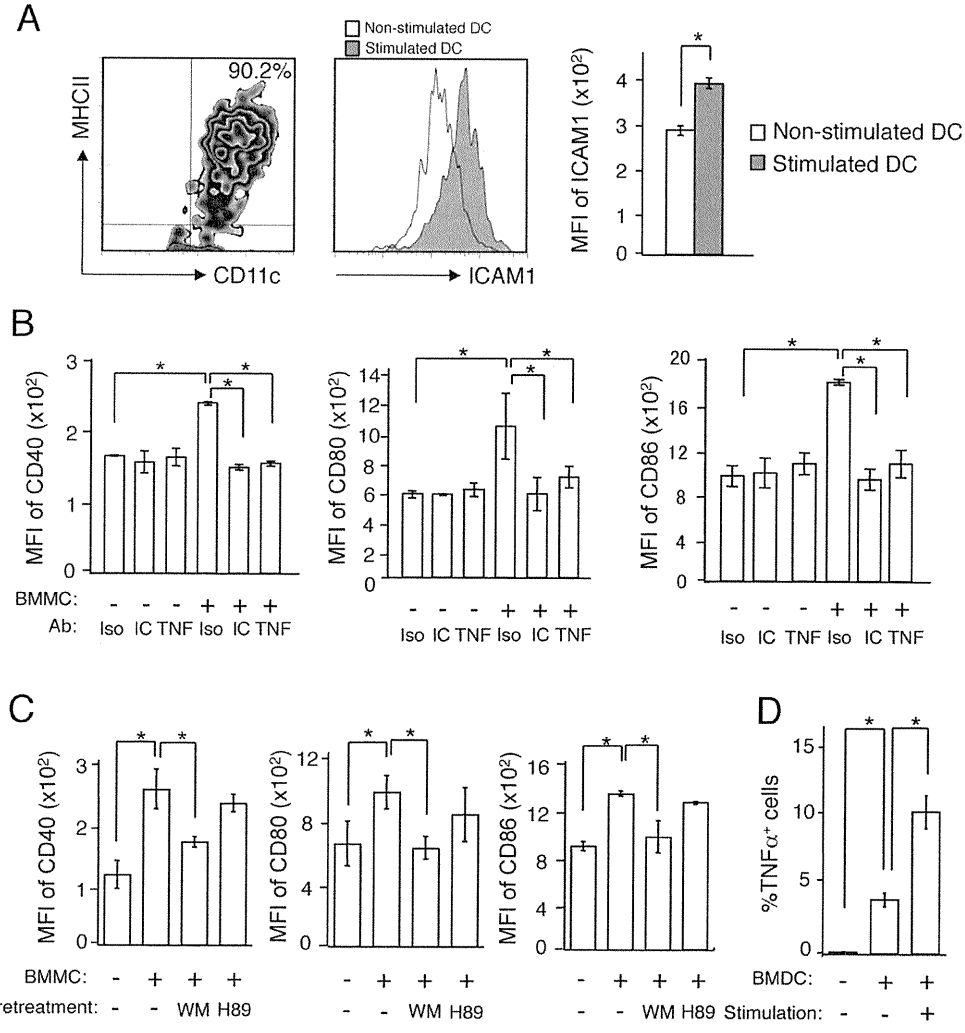

Figure 5. DC stimulation depends on ICAM-1-LFA-1 signals and membrane-bound TNF-α on MCs. (A) The expression of ICAM-1 on stimulated or non-stimulated BMDCs. (B, C) The expression levels of CD40, CD80, and CD86 on BMDCs co-cultured with BMMCs with isotype control Ab (Iso), anti-ICAM-1 Ab (IC), or anti-TNF-α Ab (TNF) (B), or co-cultured with BMMCs that were pretreated with or without wortmannin (WM) or H89 (C). (D) BMMCs expressing membrane-bound TNF-α in the presence of absence of BMDCs with or without stimulation with 100 ng/ml of LPS and 50 ng/ml of CCL21 for 1 h. All data are presented as the mean ± SD and are representative of three experiments. *, $P<0.05$.
doi:10.1371/journal.pone.0025538.g005

hapten. It is intriguing to evaluate this recovery by means of reconstitution with native skin MCs, since freshly generated BMMC and native skin MCs can differ in aspects of phenotype and function. We can't perform long term engraftment of BMMC in this model because we have found that repeated DT treatment (more than 5 days of daily injection) leads to weak viability of the Mas TRECK Tg mice.

We showed that co-culture of DCs with MCs did not promote soluble TNF-α secretion from MCs but up-regulated membrane-bound TNF-α on MCs. Since TNF-α expressed on MCs in this context is membrane-bound, MCs are required to co-localize with DCs *in vivo* to elicit its effect. Since neutralizing anti-TNF-α Ab abrogated the BMMC-induced DC maturation, membrane-bound TNF-α on MCs might be the major modulator of DC maturation. Herein we have focused on the roles of MCs in the sensitization phase, but we also noted that MC depletion in the elicitation phase attenuated the CHS response. Since DCs are thought to present antigen to memory T cells to initiate the challenge phase of CHS, the interaction of MCs and DCs might be essential for its establishment, which is a question that will be pursued in a future study.

The direct interaction between DCs and MCs was essential not only for DC stimulation, but also for MC activation. Previous reports have demonstrated that MCs contact extracellular matrix components to provide a co-stimulatory signal for histamine and cytokine production via integrins [27]. MCs are known to degranulate upon binding of ICAM-1 on MCs and LFA-1 on activated T cells [28]. In agreement with this, our study demonstrates that the interaction of MCs with DCs is dependent on cell-cell contact via ICAM-1 and LFA-1. In addition, an influx of calcium in MCs is induced by activated DCs that express high levels of ICAM-1, but not by immature DCs. Therefore, in sensitized skin, activated DCs bind to MCs and promote activation and up-regulating membrane-bound TNF-α on MCs. Activated MCs further promote additional activation of hapten-bearing cutaneous DCs causing them to migrate into skin-draining LNs. These findings indicate that MCs play an essential role in

establishing the sensitization phase of CHS by promoting cutaneous DC functions.

Materials and Methods

Mice

Mice expressing the human DTR under the control of IE element (for Mas-TRECK) and 3′UTR element (for Bas-TRECK) in the *Il4* locus were generated by a transgenic strategy. The basic pIL-4 construct was made by insertion of the 5′enhancer (5′E) (−863 to −5448; start codon is defined as sequence number 0) [29] and the IL-4 promoter from position −64 to −827. Human DTR fragment was isolated from human DTR/pMS7 vector that was provided by Dr. M. Tanaka (RCAI, RIKEN, Yokohama, Japan) and inserted into the basic pIL-4 construct. IE (+311 to +3534) and 3′UTR (+6231 to +10678) fragments were isolated from a mouse YAC clone (catalog no. 95022; Research Genetics, Huntsville, AL) and inserted into the basic pIL-4 and human DTR construct respectively. Each transgenic (Tg) line was generated on a C57BL/6 background. C57BL/6 (B6, WT) mice were purchased from Japan SLC (Shizuoka, Japan). TNF-α KO mice on the C57BL/6 background were generated [30]. WBB6F1-*Kit*+/+ and −*Kit* $^{W/W^v}$ mice were obtained from The Jackson Laboratory. For DT treatment, mice were injected intraperitoneally with 250 ng of DT in 250 µl of PBS per mouse for five consecutive days. Eight to ten week-old female mice were used for all the experiments and bred in specific pathogen-free facilities at Kyoto University. All experimental procedures were approved by the institutional animal care and use committee of Kyoto University Graduate School of Medicine (MedKyo11100).

Reagents, antibodies and intracellular staining

We purchased dinitrofluorobenzene (DNFB) from Nacalai Tesque (Kyoto, Japan), 2,4- dinitrobenzene sulfonic acid (DNBS) from Alfa Aesar (Ward Hill, MA). FITC-, PE-, PE-Cy5-, PE-Cy7-, APC-, APC-7-, and Pacific Blue-conjugated 145-2C11 (anti-CD3), GK1.5 (anti-CD4), 53-6.7 (anti-CD8), N418 (anti-CD11c), 1C10 (anti-CD40), 30-F11 (anti-CD45), 16-10A1 (anti-CD80), GL1 (anti-CD86), M5/114.15.2 (anti-MHC class II), MEL-14 (anti-CD62L), IM7 (anti-CD44), eBioKAT-1 (anti-intercellular adhesion molecule 1 (ICAM-1)), eBioL31 (anti-CD207), RB6-8C5 (anti-Gr-1), 4B12 (anti-CCR7)(eBioscience, San Diego, CA), and G8.8 (anti-EpCAM) (BioLegend, San Diego, CA) were purchased.

For Langerin (CD207) staining, cells were fixed and permeabilized with cytofix/cytoperm solution (BD Biosciences, San Jose, CA), and stained with biotin-conjugated anti-Langerin Ab. Cells were analyzed with FACSCantoII (BD, Franklin Lakes, NJ).

Histology and immunohistochemistry

Hematoxylin-eosin and toluidine blue staining [31], and the histological scoring were evaluated as reported [19]. In brief, samples were scored for the severity and character of the inflammatory response using a subjective grading scale. Responses were graded as follows: 0, no response; 1, minimal response; 2, mild response; 3, moderate response; and 4, marked response. The slides were blinded, randomized, and reread to determine the histology score. All studies were read by the same pathologist using the same subjective grading scale. The total histology score was calculated as the sum of scores, including inflammation, neutrophils, mononuclear cells, edema, and epithelial hyperplasia.

For immunohistochemistry, cryosections were fixed in acetone, incubated with hamster anti–mouse CD11c (eBioscience) followed by goat anti–hamster AlexaFluor488 (Invitrogen, Carlsbad, CA), and were subsequently incubated with PE-conjugated anti–mouse FcεRIα (eBioscience). Fluorescence images with DAPI staining were obtained using a BIOREVO BZ-9000 system (Keyence, Osaka, Japan).

Quantitative PCR analysis

Total RNAs were isolated with Trizol (Invitrogen) from ear skin. cDNA was reverse transcribed using a PrimeScript RT reagent kit (Takara Bio, Otsu, Japan). Quantitative RT-PCR with a Light Cycler real time PCR apparatus was performed (Roche Diagnostics, Foster City, CA) using SYBR Green I (Takara Bio). Primers for *Ifng*, *Il17*, and *Il1b* were obtained from Hokkaido System Science (Sapporo, Japan) and the primer sequences were *Ifng*, 5′- ATG AAC GCT ACA CAC TGC ATC -3′ (Forward) and 5′- CCA TCC TTT TGC CAG TTC CTC -3′ (reverse); *Il17*, 5′- TTT AAC TCC CTT GGC GCA AAA -3′ (forward), 5′- CTT TCC CTC CGC ATT GAC AC -3′ (reverse); and *Il1b*, 5′- GCA ACT GTT CCT GAA CTC AAC T -3′ (forward), 5′- ATC TTT TGG GGT CCG TCA ACT -3′ (reverse). For each sample, triplicate test reactions and a control reaction lacking reverse transcriptase were analyzed for expression of the genes and results were normalized to those of the 'housekeeping' glyceraldehyde-3-phosphate dehydrogenase (*Gapdh*) levels.

Lymphocyte proliferation assay and cytokine production

For DNBS-dependent proliferation, single-cell suspensions from skin-draining LNs of mice 5 days after sensitization with DNFB. One million LN cells were cultured with or without 100 µg/ml of DNBS for 72 h, pulsed with 0.5 µCi 3H-thymidine for the last 24 h, and subjected to liquid scintillation counting.

For measurement of cytokine production, the culture supernatants were collected 72 h after incubation and were measured by ELISA (BD Biosciences and R&D systems, Minneapolis, MN) according to the manufacture's protocol.

CHS protocol

Mice were sensitized with 50 µl of 0.5% (w/v) DNFB in acetone/olive oil (4/1) or 2% oxazolone (Wako Pure Chemical Industries, Ltd, Osaka, Japan) in ethanol on abdominal skin. On day 5, the ears were challenged by application of 20 µl of 0.3% DNFB or 1% oxazolone.

For adoptive transfer, LN cells were prepared from the inguinal and axillary LNs of one mouse sensitized with DNFB 5 days previously, and transferred intravenously into a mouse. The ears of these animals were challenged with 20 µl of 0.3% DNFB 1 h later, and the ear thickness change was measured. For adoptive transfer of T cells, T cells purified with CD90.2$^+$ microbeads (Miltenyi Biotec, Bergisch Gladbach, Germany) were prepared from the inguinal and axillary LNs of a mouse sensitized with 2% oxazolone 5 days previously, and transferred intravenously into a mouse. The ears of these animals were challenged with 20 µl of 1% oxazolone 1 h later, and the ear thickness change was measured.

Generation of BMDC and BMMC

Complete RPMI (cRPMI), RPMI 1640 medium (Sigma, St. Louis, MO) containing 10% fetal calf serum (Invitrogen), was used as culture medium. For BMDC induction, 5×10^6 BM cells were cultured supplemented with 10 ng/ml recombinant murine GM-CSF (PeproTech, Rocky Hill, NJ) for five days [20] (>90% expressed CD11c).

For BMMC induction, 1×10^6 BM cells were cultured supplemented with 5 ng/ml recombinant murine SCF and IL-3 (PeproTech) for more than three weeks (>98% expressed c-kit and FcεRIα).

For organ culture assay, the skin from mouse ears was split along with cartilage, and the dorsal ear skin without cartilage was floated in a dermal side-down manner in 24-well tissue culture plates. Twenty-four hours later, the cells in the wells were collected for analysis.

Chemotaxis assay and FITC-induced cutaneous DC migration

Cells were tested for transmigration to CCL21 (R&D Systems) or medium in the lower chamber across uncoated 5-μm transwell filters (Corning Costar Corp., Corning, NY) for 6 h and were enumerated by flow cytometry.

For FITC-induced cutaneous DC migration, mice were painted on the shaved abdomen with 100 μl of 2% FITC (Sigma) dissolved in a 1:1 (v/v) acetone/dibutyl phthalate (Sigma) mixture, and the number of migrated cutaneous DCs into draining LNs was enumerated by flow cytometry.

Co-culture of BMDCs and BMMCs

BMDCs and starved BMMCs were co-cultured at a density of 2×10^5 DCs in 200 μl per well in a 96-well microplate at a DC:MC ratio of 2:1 and the co-culture was performed for 24 h. Separation of BMDCs and BMMCs was performed by using transwell culture plates with a 3-μm pore size (Costar, Corning). To observe cell-cell contact *in vitro*, BMDCs and BMMCs were co-cultured on poly-L-lysine coated glass coverslips (ASAHI GLASS Co., LTD, Tokyo, Japan) for 24 h and stained with FITC-conjugated anti-c-Kit and PE-conjugated anti-MHC class II.

For inhibition assays, BMDCs and starved BMMCs were co-cultured with or without 5 μg/ml of isotype control Ab (Rat IgG2b, eBioscience), 20 μg/ml of anti-ICAM-1 Ab (YN1/1.7.4, eBioscience) or 5 μg/ml of anti-TNF-α Ab (MP6-XT22, eBioscience) for 24 h. Starved BMMCs were pretreated with or without wortmannin (100 nM; Sigma) or H89 (10 mM; Sigma) for 1 h and then co-cultured with BMDCs for 24 h.

For detection of membrane-bound TNF-α, starved BMMCs were cultured for 24 h with or without non-stimulated or stimulated BMDCs with 100 ng/ml of LPS (Sigma) and 50 ng/ml of CCL21 (R&D systems) for 1 h.

Cytoplasmic Ca^{2+} imaging

BMMCs were incubated with 5 mM Quest Fluo-8 AM (ABD Bioquest, CA, USA), and BMDCs were stimulated with 100 ng/ml of LPS and 50 ng/ml of CCL21 for 1 h and stained with 2.5 nM tetramethylrhodamine ethyl ester (TMRE) (Invitrogen). The Fluo-8 image and the transmission image were recorded every 10 sec using a back-thinned electron multiplier CCD camera (ImagEM, Hamamatsu Photonics, Japan) and microscope (Eclipse Ti, Nikon, Japan). The fluorescence intensity was expressed as a ratio to the initial value after subtracting background fluorescence.

Statistical analysis

Unless otherwise indicated, data are presented as the means ± standard deviation (SD) and are a representative of three independent experiments. *P*-values were calculated with the two-tailed Student's *t*-test or one-way ANOVA followed by the Dunnett multiple comparison test. *P* values less than 0.05 are considered to be significantly different between MasTRECK and corresponding WT mice and are shown as * in the figures.

Supporting Information

Figure S1 Effect of DT on MC in Mas-TRECK Tg mice. (A) Skin MCs in Mas-TRECK Tg mice were stained with toluidine blue with (left panel) or without (right panel) DT treatment. The numbers of skin MCs in Mas-TRECK Tg mice with or without DT treatment under steady state or inflammatory conditions (after 24 hours CHS response) are shown (lower). n.d., not detected (n = 5). (B) WT and Mas-TRECK Tg mice ($n = 5$) were treated with DT, and DCs ($CD11c^+$), B cells ($B220^+$), NK cells ($DX5^+$ $Fc\varepsilon RI^-$), NKT cells ($CD3^+DX5^+$), $CD4^+$ T cells ($CD3^+CD4^+$), $CD8^+$ T cells ($CD3^+CD8^+$), eosinophils and neutrophils ($Gr\text{-}1^+$) were obtained from PBMCs 12 days later (left). WT and Mas-TRECK Tg mice ($n = 5$) were treated with DT, and the numbers of basophils ($DX5^+Fc\varepsilon RI^+$) per ml in PBMCs were evaluated 5 days and 12 days later (right). All data are presented as the mean ± SD and are representative of three experiments.
(PDF)

Figure S2 CHS responses in *Kit* $^{W/Wv}$ and Bas-TRECK mice. (A) DNFB-induced CHS in WBB6F1-*Kit*+/+ and WBB6F1-*Kit* *Kit* $^{W/Wv}$ mice. WBB6F1-*Kit*+/+ and WBB6F1-*Kit* *Kit* $^{W/Wv}$ mice were sensitized with or without DNFB and the ear swelling was measured 24 and 48 h after challenge with DNFB ($n = 10$ per group). (B) DNFB-induced CHS in DT-treated WT and Bas-TRECK Tg mice. DT-treated WT and Bas-TRECK Tg mice were sensitized with or without DNFB and the ear swelling was measured 24 and 48 h after challenge with DNFB ($n = 10$ per group). (C) Oxazolone-induced CHS in DT-treated WT and Mas-TRECK Tg mice. Mice were sensitized with 5% oxazolone and challenged with 1% oxazolone at the high hapten dose ($n = 10$ per group). (D) CHS induced by adoptive transfer of $CD90.2^+$ T cells from WT and Mas-TRECK Tg mice sensitized with DNFB ($n = 6$ per group). (E) Toluidine blue positive mast cells in the skin with Mas TRECK Tg mice or B6 wild type mice after one hour injection of BMMC (n = 3). All data are presented as the mean ± SD and are representative of three experiments. *, $P<0.05$ versus a corresponding group.
(PDF)

Figure S3 Decreased infiltrating cells and cytokines in the skin of Mas-TRECK Tg mice after challenge. (A) The numbers of $CD4^+$ T cells, $CD8^+$ T cells and neutrophils ($CD45^+Gr\text{-}1^{high}$) in DNFB-challenged skin were counted in DT-treated Mas-TRECK Tg or WT mice ($n = 5$ per group) using flow cytometry. (B) mRNA levels of IFN-γ, IL-17 and IL-1β in the skin after CHS ($n = 5$ per group). All data are presented as the mean ± SD and are representative of three experiments.
(PDF)

Figure S4 Impaired development of the Th1 subset in CHS and decreased cytokine production in the LN of sensitized Mas-TRECK Tg mice. (A) Skin-draining LN cells were collected from MaS TRECK Tg and WT mice 5 days after DNFB application. The numbers of $CD44^{high}CD62L^+$central memory (CM) or $CD44^{high}CD62L^-$ effector memory (EM) cells and total $CD4^+$ and $CD8^+$ T cells in the draining LNs with or without sensitization are shown. (B-D) DNBS-induced lymphocyte proliferation (B) and cytokine production (C, D). Cells were collected from MaS TRECK Tg and WT mice 5 days after DNFB application and cultured for 3 days with or without 100 μg/mL DNBS. Cell proliferation was measured by ^3H-thymidine incorporation. The amounts of IFN-γ and IL-17 in the culture medium were measured by ELISA. $n = 10$ mice per group.
(PDF)

Figure S5 Attenuated DC maturation in the absence of MCs. (A) Representative flow cytometry profiles of the skin from WT and Mas TRECK Tg mice (left), and histogram of CD40 expression on LCs and dDCs from DT-treated WT mice and Mas-TRECK Tg mice treated with or without DT. (B) The

expression levels of CD40, CD80, and CD86 on LCs and dDCs in the ear skin from WBB6F1-*Kit*+/+, -*Kit* $^{W/Wv}$,WT, and Mas-TRECK Tg mice under steady state conditions.
(PDF)

Figure S6 timulation of DCs by MCs is dependent on ICAM-1-LFA-1 interaction and on MC membrane-bound TNF-α. (A, B) Histogram. The expression levels of CD40 on BMDCs co-cultured with BMMCs with isotype control Ab, anti-ICAM-1 Ab, or anti-TNF-α Ab (TNF) (A), or co-cultured with BMMCs that were pretreated with or without wortmannin (WM) or H89 (B). (C) The expression levels of CD40, CD80, and CD86 on BMDCs co-cultured with WT derived BMMCs or TNF-α KO (TNF KO) derived BMMCs.
(PDF)

Video S1 Quest Fluo-8 AM-stained BMMCs and TMRE-stained BMMCs were mixed on glass coverslips and recorded every 10 sec at ~30°C using a back-thinned electron multiplier CCD camera.
(MOV)

Video S2 Quest Fluo-8 AM-stained BMMCs and TMRE-stained stimulated BMMCs were mixed on glass coverslips and recorded every 10 sec at ~30°C using a back-thinned electron multiplier CCD camera.
(MOV)

Acknowledgments

We thank Dr. Heinrich Körner (Cellular Immunology Laboratory, Comparative Genomics Centre, James Cook University, Townsville, 4811, Queensland, Australia) and Dr. Hajime Suto (Atopy Research Center, Juntendo University School of Medicine, Tokyo, 113-8412, Japan) for kindly providing TNF-α KO mice.

Author Contributions

Conceived and designed the experiments: AO MK. Performed the experiments: AO BK SM. Analyzed the data: TH GE SN HT TW SN. Contributed reagents/materials/analysis tools: MK. Wrote the paper: YM KK.

References

1. Grabbe S, Schwarz T (1998) Immunoregulatory mechanisms involved in elicitation of allergic contact hypersensitivity. Immunol Today 19: 37–44.
2. Tomura M, Honda T, Tanizaki H, Otsuka A, Egawa G, et al. (2010) Activated regulatory T cells are the major T cell type emigrating from the skin during a cutaneous immune response in mice. J Clin Invest 120: 883–893.
3. Egawa G, Honda T, Tanizaki H, Doi H, Miyachi Y, et al. (2011) In Vivo Imaging of T-Cell Motility in the Elicitation Phase of Contact Hypersensitivity Using Two-Photon Microscopy. J Invest Dermatol.
4. Egawa G, Kabashima K (2011) Skin as a Peripheral Lymphoid Organ: Revisiting the Concept of Skin-Associated Lymphoid Tissues. J Invest Dermatol.
5. Kabashima K, Miyachi Y (2004) Prostanoids in the cutaneous immune response. J Dermatol Sci 34: 177–184.
6. Romani N, Clausen BE, Stoitzner P (2010) Langerhans cells and more: langerin-expressing dendritic cell subsets in the skin. Immunol Rev 234: 120–141.
7. Bursch LS, Wang L, Igyarto B, Kissenpfennig A, Malissen B, et al. (2007) Identification of a novel population of Langerin+ dendritic cells. J Exp Med 204: 3147–3156.
8. Honda T, Nakajima S, Egawa G, Ogasawara K, Malissen B, et al. (2010) Compensatory role of Langerhans cells and langerin-positive dermal dendritic cells in the sensitization phase of murine contact hypersensitivity. J Allergy Clin Immunol 125: 1154–1156 e1152.
9. Kitawaki T, Kadowaki N, Sugimoto N, Kambe N, Hori T, et al. (2006) IgE-activated mast cells in combination with pro-inflammatory factors induce Th2-promoting dendritic cells. Int Immunol 18: 1789–1799.
10. Jawdat DM, Albert EJ, Rowden G, Haidl ID, Marshall JS (2004) IgE-mediated mast cell activation induces Langerhans cell migration in vivo. J Immunol 173: 5275–5282.
11. Suto H, Nakae S, Kakurai M, Sedgwick JD, Tsai M, et al. (2006) Mast cell-associated TNF promotes dendritic cell migration. J Immunol 176: 4102–4112.
12. Kabashima K, Narumiya S (2003) The DP receptor, allergic inflammation and asthma. Prostaglandins Leukot Essent Fatty Acids 69: 187–194.
13. Hammad H, de Heer HJ, Soullie T, Hoogsteden HC, Trottein F, et al. (2003) Prostaglandin D2 inhibits airway dendritic cell migration and function in steady state conditions by selective activation of the D prostanoid receptor 1. J Immunol 171: 3936–3940.
14. Galli SJ, Hammel I (1984) Unequivocal delayed hypersensitivity in mast cell-deficient and beige mice. Science 226: 710–713.
15. Galli SJ, Grimbaldeston M, Tsai M (2008) Immunomodulatory mast cells: negative, as well as positive, regulators of immunity. Nat Rev Immunol 8: 478–486.
16. Yu N, Zhang S, Zuo F, Kang K, Guan M, et al. (2009) Cultured human melanocytes express functional toll-like receptors 2-4, 7 and 9. J Dermatol Sci 56: 113–120.
17. Swope VB, Sauder DN, McKenzie RC, Sramkoski RM, Krug KA, et al. (1994) Synthesis of interleukin-1 alpha and beta by normal human melanocytes. J Invest Dermatol 102: 749–753.
18. Yagi R, Tanaka S, Motomura Y, Kubo M (2007) Regulation of the Il4 gene is independently controlled by proximal and distal 3′ enhancers in mast cells and basophils. Mol Cell Biol 27: 8087–8097.
19. Nakajima S, Honda T, Sakata D, Egawa G, Tanizaki H, et al. (2010) Prostaglandin I2-IP signaling promotes Th1 differentiation in a mouse model of contact hypersensitivity. J Immunol 184: 5595–5603.
20. Tanizaki H, Egawa G, Inaba K, Honda T, Nakajima S, et al. (2010) Rho-mDia1 pathway is required for adhesion, migration, and T-cell stimulation in dendritic cells. Blood 116: 5875–5884.
21. Chang WC, Nelson C, Parekh AB (2006) Ca2+ influx through CRAC channels activates cytosolic phospholipase A2, leukotriene C4 secretion, and expression of c-fos through ERK-dependent and -independent pathways in mast cells. Faseb J 20: 2381–2383.
22. Cella M, Scheidegger D, Palmer-Lehmann K, Lane P, Lanzavecchia A, et al. (1996) Ligation of CD40 on dendritic cells triggers production of high levels of interleukin-12 and enhances T cell stimulatory capacity: T-T help via APC activation. J Exp Med 184: 747–752.
23. Black RA, Rauch CT, Kozlosky CJ, Peschon JJ, Slack JL, et al. (1997) A metalloproteinase disintegrin that releases tumour-necrosis factor-alpha from cells. Nature 385: 729–733.
24. Kriegler M, Perez C, DeFay K, Albert I, Lu SD (1988) A novel form of TNF/cachectin is a cell surface cytotoxic transmembrane protein: ramifications for the complex physiology of TNF. Cell 53: 45–53.
25. Bryce PJ, Miller ML, Miyajima I, Tsai M, Galli SJ, et al. (2004) Immune sensitization in the skin is enhanced by antigen-independent effects of IgE. Immunity 20: 381–392.
26. Piliponsky AM, Chen CC, Grimbaldeston MA, Burns-Guydish SM, Hardy J, et al. (2010) Mast cell-derived TNF can exacerbate mortality during severe bacterial infections in C57BL/6-KitW-sh/W-sh mice. Am J Pathol 176: 926–938.
27. Ra C, Yasuda M, Yagita H, Okumura K (1994) Fibronectin receptor integrins are involved in mast cell activation. J Allergy Clin Immunol 94: 625–628.
28. Inamura N, Mekori YA, Bhattacharyya SP, Bianchine PJ, Metcalfe DD (1998) Induction and enhancement of Fc(epsilon)RI-dependent mast cell degranulation following coculture with activated T cells: dependency on ICAM-1- and leukocyte function-associated antigen (LFA)-1-mediated heterotypic aggregation. J Immunol 160: 4026–4033.
29. Kubo M, Ransom J, Webb D, Hashimoto Y, Tada T, et al. (1997) T-cell subset-specific expression of the IL-4 gene is regulated by a silencer element and STAT6. EMBO J 16: 4007–4020.
30. Korner H, Cook M, Riminton DS, Lemckert FA, Hoek RM, et al. (1997) Distinct roles for lymphotoxin-alpha and tumor necrosis factor in organogenesis and spatial organization of lymphoid tissue. Eur J Immunol 27: 2600–2609.
31. Maurer M, Fischer E, Handjiski B, von Stebut E, Algermissen B, et al. (1997) Activated skin mast cells are involved in murine hair follicle regression (catagen). Lab Invest 77: 319–332.

Multiple Follicular Pustules as an Atypical Cutaneous Manifestation of Drug-induced Hypersensitivity Syndrome

Yuri Ueharaguchi[1,2]*, Kenji Kabashima[2]*, Chihiro Shimizuhira[1], Wataru Nakajo[3], Takeshi Kondo[3], Toru Kamiya[3], Kunihiko Matsubara[4] and Setsuko Kondo[1]

*Departments of [1]Dermatology, [3]General Internal Medicine, and [4]Wound Healing Center, Rakuwakai Otowa Hospital, Kyoto, and [2]Department of Dermatology, Kyoto University Graduate School of Medicine, 54 Shogoin-Kawara, Sakyo, Kyoto 606-8507, Japan. *E-mail: yuriguchi823@hotmail.com, kaba@kuhp.kyoto-u.ac.jp*

Accepted March 16, 2011.

Drug-induced hypersensitivity syndrome (DIHS), also known as drug rash with eosinophilia and systemic symptoms (DRESS), is a severe drug reaction presenting with generalized skin eruption, organ failure and haematological abnormality (1, 2). Typical cutaneous manifestations include maculopapular, lichenoid, purpuriform, target-like and possibly also other types of lesions. Erythroderma with or without exfoliation or desquamation may sometimes be observed. We report here a case of DIHS/DRESS presenting with multiple diffuse follicular pustules on the trunk and extremities.

CASE REPORT

A 15-year-old Japanese male student was admitted to our hospital with generalized pruritic rash and high fever after treatment with carbamazepine for epilepsy over 5 weeks. The patient exhibited marked oedema on the face (Fig. 1A), cervical lymphadenopathy, and small follicular pustules diffusely distributed on his trunk and extremities (Fig. 1B). Bacterial cultures of both blood and pustules were negative. A skin biopsy from the back revealed a spongiotic pustule in the follicular infundibulum with moderate upper-dermal perivascular infiltrations of lymphocytes, neutrophils and a few eosinophils (Fig. 1C). A blood test indicated leukocytosis (white blood cell count, 12,000/ml) containing up to 5% atypical lymphocytes, marked eosinophilia (2,280/ml), elevated levels of liver enzymes (aspartate aminotransferase (AST) 367 IU/l and alanine aminotranferase (ALT) 1,637 IU/l), and positivity for human herpes virus (HHV)-6 DNA. Treatment with 30 mg oral prednisone resulted in improvement in the patient's general condition and skin eruptions.

DISCUSSION

This case fulfils the criteria for both DIHS (7/7 of the Japanese consensus group criteria) and DRESS (8/9 of the Kardaun et al. criteria (7)) (Table I). The mechanism of DIHS/DRESS has not been fully elucidated. Immune responses by drug-reactive T cells, plasmacytoid dendritic cells, and activation of herpes viruses have been proposed (2, 3).

Before the concept of DIHS/DRESS was established, anticonvulsant hypersensitivity syndrome was recognized as a severe adverse drug reaction induced by anticonvulsants such as carbamazepine, phenytoin,

Fig. 1. Clinical and histological findings in a patient with drug-induced hypersensitivity syndrome/drug rash with eosinophilia and systemic symptoms. (A and B) Clinical manifestations. The patient had marked oedema of the face and small, diffusely distributed, follicular pustules. (C) Histological examination revealed a spongiotic pustule in the follicular infundibulum with moderate upper-dermal perivascular infiltrations.

Table I. *Criteria for drug-induced hypersensitivity syndrome (DIHS; top) and drug rash with eosinophilia and systemic symptoms (DRESS; bottom). The patient met the criteria for DIHS (7/7) and DRESS (8/9)*

Criteria for typical DIHS (presence of all 7 criteria) (ref. 6)

1. HHV-6 reactivation
2. Prolonged clinical symptoms 2 weeks after discontinuation of causative drug
3. Maculopapular rash developing > 3 weeks after starting with limited number of drugs
4. Fever > 38°C
5. Lymphadenopathy
6. Liver abnormalities (alanine aminotransferase > 100 U/l) or other organ involvement, e.g. renal involvement
7. Leukocyte abnormalities (at least one present)
   - Leukocytosis ($> 11 \times 10^9$/l)
   - Atypical lymphocytosis (> 5%)
   - Eosinophilia ($> 1.5 \times 10^9$/l)

	Score –1	Score 0	Score 1	Score 2
*Scoring system for classifying DRESS cases as definite, probable, possible, or no case[a] (applicable items in **bold**) (ref. 7)*				
Fever ≥ 38.5°C	No/U	**Yes**		
Enlarged lymph node		No/U	**Yes**	
Eosinophilia		No/U		
Eosinophils			$0.7–1.499 \times 10^9 l^{-1}$	$\mathbf{\geq 1.5 \times 10^9 l^{-1}}$
Eosinophils, if leucocytes $< 4.0 \times 10^9 l^{-1}$			10–19.9%	≥ 20%
Atypical lymphocytes		No/U	**Yes**	
Skin involvement				
Skin rash extent (% body surface area)		No/U	**≥ 50%**	
Skin rash suggesting DRESS	No	U	**Yes**	
Biopsy suggesting DRESS	No	Yes/U		
Organ involvement				
Liver, kidney, lung, muscle/heart, pancreas, other organ			**One organ**	Two or more organ
Resolution ≥ 15 days	No/U	**Yes**		
Evaluation of other potential causes				
Antinuclear antibody				
Blood culture				
Serology for HAV/HBV/HCV				
Chlamydia/mycoplasma				
If none positive and ≥ 3 of above negative			**Yes**	

[a]Total score < 2: no case; 2–3; possible case; 4–5: probable case; > 5: definite case.
U: unknown/unclassifiable; HAV: hepatitis A virus; HBV: hepatitis B virus; HCV: hepatitis C virus; HHV-6: human herpes virus 6.

and phenobarbital sodium (4). Several cases of acute generalized exanthematous pustulosis (AGEP) induced by anticonvulsants have been reported (5), but isolated pustules in the follicular infundibulum, as seen in our case, are a clear contrast to AGEP, which usually manifests histopathologically as confluent, flaccid pustules with non-follicular, subcorneal or upper-epidermal pustules.

We diagnosed the patient as typical DIHS, since we observed the reactivation of HHV-6 in addition to the clinical manifestations seen in DRESS. The case was diagnosed as DIHS/DRESS with reactivation of HHV-6. We describe here an atypical case of DIHS presenting with diffuse follicular pustules on the trunk and extremities, which was reasonably well controlled by conventional therapy with an oral steroid.

REFERENCES

1. Bocquet H, Bagot M, Roujeau JC. Drug-induced pseudolymphoma and drug hypersensitivity syndrome (drug rash with eosinophilia and systemic symptoms: DRESS). Semin Cutan Med Surg 1996; 15: 250–257.
2. Shiohara T, Kano Y. A complex interaction between drug allergy and viral infection. Clin Rev Allergy Immunol 2007; 33: 124–133.
3. Sugita K, Tohyama M, Watanabe H, Otsuka A, Nakajima S, Iijima M, et al. Fluctuation of blood and skin plasmacytoid dendritic cells in drug-induced hypersensitivity syndrome. J Allergy Clin Immunol 2010; 126: 408–410.
4. Shear NH, Spielberg SP. Anticonvulsant hypersensitivity syndrome. In vitro assessment of risk. J Clin Invest 1988; 82: 1826–1832.
5. Son CH, Lee CU, Roh MS, Lee SK, Kim KH, Yang DK. Acute generalized exanthematous pustulosis as a manifestation of carbamazepine hypersensitivity syndrome. J Investig Allergol Clin Immunol 2008; 18: 461–464.
6. ShioharaT, Iijima M, Ikezawa Z, Hashimoto K. The diagnosis of a DRESS syndrome has been sufficiently established on the basis of typical features and viral reactivations. Br J Dermatol 2007; 156: 1083–1084.
7. Kardaun SH, Sidoroff A, Valeyrie-Allanore L, Halevy S, Davidovici BB, Mockenhaupt M, et al. Variability in the clinical pattern of cutaneous side-effects of drugs with systemic symptoms: does a DRESS syndrome really exist? Br J Dermatol 2007; 156: 609–611.

Journal of Dermatological Science xxx (2011) xxx–xxx

Contents lists available at SciVerse ScienceDirect

Journal of Dermatological Science

journal homepage: www.elsevier.com/jds

The predominant drug-specific T-cell population may switch from cytotoxic T cells to regulatory T cells during the course of anticonvulsant-induced hypersensitivity

Takaaki Hanafusa, Hiroaki Azukizawa *, Sayaka Matsumura, Ichiro Katayama

Department of Dermatology, Osaka University Graduate School of Medicine, 2-2 Yamadaoka, Suita-shi, Osaka 565-0871, Japan

ARTICLE INFO

Article history:
Received 24 August 2011
Received in revised form 22 November 2011
Accepted 2 December 2011

Keywords:
Drug allergy
Adverse drug reaction
Immunologic tests
In vitro tests
Immunology

ABSTRACT

Background: Delayed hypersensitivity is responsible for severe cutaneous adverse drug reactions (cADRs), especially in Stevens-Johnson syndrome (SJS), toxic epidermal necrolysis, and drug-induced hypersensitivity syndrome (DIHS) (also known as drug rash with eosinophilia and systemic symptoms [DRESS] syndrome). The drug-induced lymphocyte stimulation test (DLST), or lymphocyte transformation test (LTT), is used to identify the culprit drug in severe cADR cases.
Objective: The aim of this study was to examine the immune reactions in cADR patients through the identification of the drug-specific proliferating cells by flow cytometric DLST (FCM-DLST).
Methods: The peripheral blood mononuclear cells of 16 anticonvulsant-induced cADR patients were investigated by conventional DLST and a FCM-DLST protocol in which CFSE dilution and BrdU incorporation were combined. FCM-DLST allowed for the identification of the drug-specific proliferating cells in six cases. Three of these cases were DIHS cases, whereas there was one case of SJS, one case of maculopapular rash (MP), and one case of erythema multiforme (EM) among the six cases.
Results: In FCM-DLST, drug-specific proliferating T cells were detected as $CFSE^{low}$ $BrdU^{high}$ cells. These cells corresponded to the cells incorporating ^{3}H-thymidine in conventional DLST. Although $CD4^{+}$ T-cell proliferation dominated the observed proliferation in most of the cases (in the recovery stage of the three DIHS cases, the MP case, and the EM case), drug-specific $CD8^{+}$ cytotoxic T lymphocytes (CTLs) were detected, especially in the acute stages of the SJS case and one of the DIHS cases. There was a dramatic switch in the predominant drug-specific proliferating T-cell population in the course of one of the cases of DIHS in which $CD8^{+}$ CTLs were predominant initially, whereas $CD4^{+}$ T cells were predominant later. Moreover, drug-specific $CD4^{+}$ $CD25^{+}$ $Foxp3^{+}$ regulatory T cells (Tregs) proliferated during the recovery stage in one DIHS case.
Conclusions: FCM-DLST revealed that the cell proliferation detected by conventional DLST is a heterogeneous proliferation of both $CD8^{+}$ CTLs and $CD4^{+}$ T cells that likely includes Tregs. However, the number of cADR cases in this study was limited, which limits the conclusions that can be drawn from it.

1. Introduction

T-cell-mediated delayed hypersensitivity is responsible for the pathogenesis of severe cutaneous adverse drug reactions (cADRs), including Stevens-Johnson syndrome (SJS), toxic epidermal necrolysis (TEN), and drug-induced hypersensitivity syndrome (DIHS), also called hypersensitivity syndrome (HSS) or drug rash with eosinophilia and systemic symptoms (DRESS) syndrome [1–4]. In severe cADR, the drug-induced lymphocyte stimulation test (DLST), or lymphocyte transformation test (LTT), is used to identify culprit drugs [5]. In conventional DLST, freshly isolated peripheral blood mononuclear cells (PBMCs) are incubated with the culprit drug for 5–7 days, and cell proliferation is measured by ^{3}H-thymidine incorporation. Because ^{3}H-thymidine incorporation occurs in all proliferating PBMCs, drug-specific proliferating cells cannot be individually assessed by conventional DLST.

Flow cytometry (FCM) is a well-established semiquantitative assay that can measure the cell surface and intracellular molecules expressed by individual cells in a heterogeneous population. It has also been used for analyzing the in vitro immune reaction that occurs in DLST [6]. Drug-specific T cells and their cytokine production were detected by a carboxyfluorescein diacetate succinimidyl ester (CFSE)-based proliferation assay [7–9]. CFSE is partitioned equally during cell division, resulting in the

* Corresponding author. Tel.: +81 6 6879 3031; fax: +81 6 6879 3039.
E-mail address: azukizaw@derma.med.osaka-u.ac.jp (H. Azukizawa).

0923-1811/$36.00
doi:10.1016/j.jdermsci.2011.12.002

sequential halving of cellular fluorescent intensity with each successive generation. Although CFSE dilution is usually a useful technique for the measurement of cell proliferation, cells that have proliferated are sometimes indistinguishable from a non-specific peak of dead cells, especially when the cell proliferation is small in magnitude, which it often is in a DLST reaction. 5-bromo-2′-deoxyuridine (BrdU) is a non-radioactive thymidine analogue that becomes incorporated into DNA during the S-phase of the cell cycle (Fig. 1A). Here, drug-specific proliferating cells were identified by a flow cytometric DLST (FCM-DLST) protocol that combines CFSE dilution and BrdU incorporation and utilizes them as a substitute for ^{3}H-thymidine incorporation. The combination of the CFSE and BrdU assays allows for the clear identification of the very small proliferating cell population as $CFSE^{low}$ $BrdU^{high}$ cells. A FCM-DLST protocol that uses the combination of CFSE and BrdU assays can reveal the proliferating drug-specific cell population responsible for the proliferation found by conventional DLST. We took advantage of this feature and analyzed the drug-specific T cells of anti-convulsant hypersensitivity patients during the acute and recovery stages of the disease. Interestingly, drug-specific $CD8^{+}$ T cells were detected only in the acute stage of severe drug hypersensitivity, whereas drug-specific $CD4^{+}$ T cells were found to be dominant in the recovery stage. Moreover, the percentage of drug-specific $CD4^{+}$ T cells that were $Foxp3^{+}$ regulatory T cells (Tregs) was increased during the recovery stage in one of the DIHS cases, suggesting that different subsets of drug-specific T cells are induced during different disease stages of a cADR.

2. Materials and methods

2.1. Patients

Sixteen patients clinically diagnosed with anticonvulsant-induced cADR were enrolled in this study from July 2008 to July 2011. Conventional DLST was performed in all 16 cases, while FCM-DLST was performed in six of the cases. Our institutional review board approved this study, and informed consent for all diagnostic procedures and research was obtained from all patients and healthy controls.

2.2. Cell preparation and culture

Cell preparation and culture for DLST were performed in accordance with standard DLST protocols [6,10,11]. Briefly, PBMCs were isolated with Ficoll-Hypaque solution (Sigma–Aldrich), labeled with 6 mM CFSE (Invitrogen), and cultured at 2×10^{5} cells/well in two 96-well flat-bottomed plates for 7 days. After addition of the identified culprit drug, one plate was used for conventional DLST and one for FCM-DLST (Fig. 1B).

2.3. Preparation of culprit drugs

Culprit drugs were dissolved in phosphate-buffered saline (PBS), or PBS with 0.025% dimethyl sulfoxide (Wako) if the drug was PBS-insoluble, and added to the PBMC culture medium at the beginning of incubation (day 0). Sodium valproate was PBS-soluble, whereas phenytoin, zonisamide, and carbamazepine were PBS-insoluble. The final drug concentrations were 100, 10, and 1 μg/ml. PBMCs were also incubated without a drug (negative control) and with 10 μg/ml phytohemagglutinin (PHA, Sigma–Aldrich; positive control).

2.4. ^{3}H-thymidine incorporation assay for DLST

Conventional DLST that used ^{3}H-thymidine was performed as previously described [10,11]. The results are presented as the stimulation index (SI), which was the ratio of the highest count per minute of the samples cultured with diluted drug to that of the control cultured without a drug. A SI value >2.0 was interpreted as a positive result.

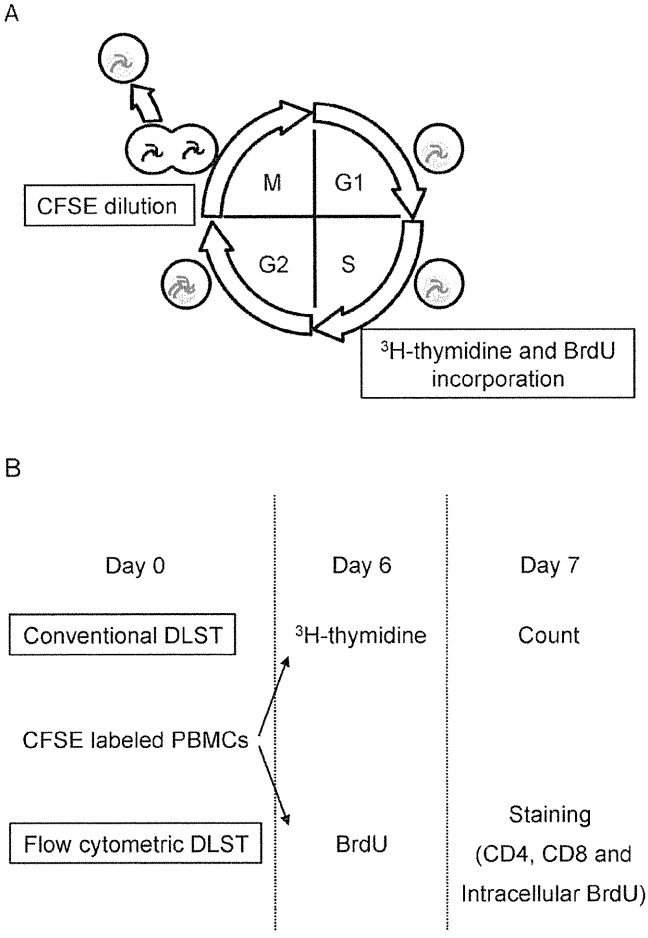

Fig. 1. (A) Cell cycle scheme. ^{3}H-thymidine and BrdU are incorporated into S-phase cells, while the CFSE intensity of a labeled cell is reduced by half every cell division. G1: gap 1 phase; S: synthesis phase; G2: gap 2 phase; M: mitotic phase; BrdU: 5-bromo-2′-deoxyuridine; CFSE: carboxyfluorescein diacetate succinimidyl ester. (B) Comparison of the conventional and flow cytometric drug-induced lymphocyte stimulation tests (DLST). A patient's peripheral blood mononuclear cells (PBMCs) were isolated and CFSE-labeled. They were cultured for 7 days in two culture plates with a culprit drug for conventional and flow cytometric DLST (one plate for conventional, one for flow cytometric). Six days after incubation, ^{3}H-thymidine or BrdU were added. After an additional 20–24 h of incubation, the cells were harvested, and ^{3}H-thymidine incorporation was measured for conventional DLST. For flow cytometric DLST, BrdU-pulsed cells were stained with anti-CD4 and anti-CD8 antibodies, fixed, permeabilized, and then intracellularly stained for BrdU.

2.5. Flow cytometric DLST

The other plate of CFSE-labeled PBMCs was incubated with or without culprit drug in the same manner (Fig. 1B). Six days after the start of incubation, 10 μm BrdU (Sigma–Aldrich) was pulsed into the wells instead of ^{3}H-thymidine. After 20–24 h of further incubation, the cells were collected and stained with the following antibodies and reagents: Peridinin chlorophyll protein (PerCP)-conjugated CD4, allophycocyanin (APC)-conjugated CD8, streptavidin–phycoerythrin (PE) (all BD Biosciences), and biotin-conjugated BrdU (Abcam). For intracellular BrdU staining, cells were labeled with CD4 and CD8, fixed and permeabilized with BD Cytofix/Cytoperm™ Fixation/Permeabilization Solution Kit (BD Biosciences), and treated with 0.3 mg/ml Deoxyribonuclease I

Please cite this article in press as: Hanafusa T, et al. The predominant drug-specific T-cell population may switch from cytotoxic T cells to regulatory T cells during the course of anticonvulsant-induced hypersensitivity. J Dermatol Sci (2012), doi:10.1016/j.jdermsci.2011.12.002